Title

Ataxin-7 and non-stop coordinate SCAR protein levels, subcellular localization, and actin cytoskeleton organization

Running Title

SCAR is regulated by Atxn7 and non-stop

Authors

Veronica Cloud[1], Elaheh Momtahan[1], Jarrid L. Jack[1], Edgardo Leiva[1], Sarah Rapp[1], Sara Miller[1], Daniel Holsapple[1], Lauren G. Shelton[2], Richard A Pierce[2], Ying Zhang[2], Laurence Florens[2], Michael P Washburn[2], Ryan D. Mohan[1]*

[1]University of Missouri – Kansas City, Kansas City, MO, USA.

[2]Stowers Institute for Medical Research, Kansas City, MO, USA.

*corresponding author MohanRD@umkc.edu

Summary

SAGA subunits Atxn7 and non-stop regulate stability and subcellular localization of WRC subunit SCAR. Loss of Atxn7 increases, while loss of non-stop decreases, SCAR protein levels and F-actin network assembly.

Abstract

Ataxin-7 (Atxn7), a subunit of the SAGA transcriptional coactivator complex, is subject to polyglutamine expansion at the amino terminus, causing spinocerebellar ataxia type 7 (SCA7), a progressive retinal and neurodegenerative disease. Within SAGA, the Atxn7 amino terminus anchors the non-stop deubiquitinase to the complex. To understand the consequences of Atxn7-dependent regulation of non-stop, we sought substrates for non-stop and discovered the deubiquitinase, dissociated from SAGA, interacts with Arp2/3 and WAVE regulatory complexes (WRC). Protein levels of WRC subunit SCAR are regulated by a constant ubiquitination/proteasomal degradation mechanism. Loss of Atxn7 frees non-stop from SAGA, and increased protein levels of WRC subunit SCAR, while loss of non-stop resulted in reduced protein levels of SCAR. Proteasome inhibition fully rescued SCAR protein levels upon loss of non-stop. Dependent on conserved WRC interacting receptor sequences (WIRS), non-stop

overexpression increased SCAR protein levels and directed subcellular localization of SCAR, leading to decreased cell area and decreased number of protrusions.

Keywords: Ataxin-7, non-stop, USP22, Arp2/3, spinocerebellar ataxia type 7, SCA7, actin, WAVE regulatory complex, SAGA complex, SCAR, neural.

Introduction

The Spt Ada Gcn5 Acetyltransferase (SAGA) transcriptional coactivator complex is an approximately 1.8 MDa, modular, multi-protein complex, bearing two enzymatic subunits (Gcn5 acetyltransferase and non-stop deubiquitinase) housed in separate modules of the complex (Lee et al., 2011a). Within SAGA, the Ataxin-7 (Atxn7) amino-terminus anchors the deubiquitinase module (DUBm) to the larger complex (Lee et al., 2009). Mutation of Atxn7 and nonstop leads to aberrant gene expression, defective non-homologous end joining, decreased immune response, reduced replicative lifespan, neurodegeneration, blindness, tumorigenesis, and cancer (Bonnet et al., 2014; Furrer et al., 2011; Glinsky et al., 2005; Lang et al., 2011; Li et al., 2018; McCormick et al., 2014; Weake et al., 2008).

The progressive retinal and neurodegenerative disease Spinocerebellar Ataxia type 7 (SCA7) is caused by CAG trinucleotide repeat expansion of the *ATXN7* gene, resulting in polyglutamine (polyQ) expansion at the amino terminus of the Atxn7 protein (David et al., 1997; Giunti et al., 1999). SCA7 disease is characterized by progressive cone-rod dystrophy leading to blindness, and progressive degeneration of the spine and cerebellum (Garden, 1993; Martin, 2012).

In *Drosophila*, loss of Atxn7 leads to a phenotype similar to overexpression of the polyQ-expanded amino terminal truncation of human Atxn7 (Latouche et al., 2007) – reduced life span, reduced mobility, and retinal degeneration (Mohan et al., 2014b). Without Atxn7, the Drosophila DUBm is released, enzymatically active, from SAGA. Once released, the module acts with a gain-of-function, leading to reduced ubiquitination of H2B. Similarly, the mammalian DUBm binds and deubiquitinates substrates without Atxn7 (Lan et al., 2015; Yang et al., 2015). Consistent with non-stop release and over activity in mediating the Drosophila Atxn7 loss-of-function phenotype, reducing *non-stop* copy number alleviates lethality associated with loss of Atxn7 (Mohan et al., 2014b).

Non-stop is a critical mediator of retinal axon guidance and important for glial cell survival (Martin et al., 1995; Weake et al., 2008). Interestingly, abnormal ubiquitin signaling in

the nervous system contributes to a number of genetic and spontaneous neurological and retinal diseases, including SCA3, SCAR16, Alzheimer's, Parkinson's, ALS, and Huntington's disease (Campello et al., 2013a; Campello et al., 2013b; Mohan et al., 2014a; Petrucelli and Dawson, 2004). Few functions are known for the DUBm beyond deubiquitination of H2Bub, H2Aub, shelterin, and FBP1 (Atanassov and Dent, 2011; Atanassov et al., 2009). In polyQ-Atxn7 overexpression models, sequestration of the DUBm may result in reduced deubiquitinase activity on critical substrates. Interestingly, both increased and decreased H2Bub have been shown to hinder gene expression and imbalances (whether up or down), in ubiquitination have been observed in numerous retinal and neurological diseases (Ristic et al., 2014). Together, these data suggest more needs to be understood about Atxn7-mediated regulation of DUBm function.

We set out to identify substrates for non-stop and determine the consequence of Atxn7 loss on non-stop/substrate interactions. To this end, we purified non-stop-containing complexes, fractionated them by size, and tested enzymatic activity to identify novel complexes bearing enzymatically active non-stop. This revealed a portion of functionally active DUBm associates with protein complexes distal from SAGA. Mass spectrometry revealed Arp2/3 complex and Wiskott-Aldrich syndrome protein (WASP)-family verprolin homologous protein (WAVE) Regulatory Complex (WRC) members SCAR, HEM protein (Hem), and specifically Rac1 associated protein 1 (Sra-1), as interaction partners of the independent DUBm. These complexes function together to initiate actin branching (Kurisu and Takenawa, 2009). Pull-down and immunofluorescence verified interaction and revealed extensive colocalization between non-stop and WRC subunit SCAR.

Spatiotemporal regulation of SCAR is essential for maintaining cytoskeletal organization. A constant ubiquitination-proteasomal degradation mechanism contributes to establishing SCAR protein amount. WRC subunits HEM, SRA-1, and Abi mediate interaction with an unidentified deubiquitinase to counteract proteasomal degradation of SCAR (Kunda et al., 2003). WRC subunits Abi and SRA-1 mediate interaction with numerous proteins which bear a WIRS motif to regulate SCAR location. In cells and in flies, loss of Atxn7 resulted in a 2.5 fold increase in SCAR protein levels, suggesting released non-stop counteracts proteasomal degradation of SCAR. Accordingly, loss of non-stop led to a 70% loss of SCAR protein, which was completely rescued by proteasome inhibition. Overexpression of non-stop increased total SCAR protein levels approximately 5-fold. Interestingly, SCAR protein levels increased in cellular compartments where non-stop increased, including in the nucleus. The functional output

of SCAR is F-actin formation. When SCAR protein levels were increased and relocalized by augmenting non-stop, local F-actin amounts increased too, leading to cell rounding and fewer cell protrusions. Analysis of non-stop protein sequence revealed the presence of WIRS motifs. Mutation of these reduced non-stop ability to increase SCAR protein, F-actin, and to reduce cellular protrusions.

Results

Non-stop interacts with multi-protein complexes distal from SAGA

Loss of Atxn7, releases non-stop from SAGA resulting in a deubiquitinase gain-of-function, reducing ubiquitination of histone H2B (Mohan et al., 2014b). The resultant retinal and neurodegenerative phenotype is rescued by reducing non-stop yet it is not consistent with phenotypes arising from mutations in other regulators of H2B ubiquitination, such as Dhr6 (the E2 ubiquitin conjugating enzyme), Bre1 (E3 ubiquitin ligase), or USP7 (H2B deconjugating enzyme) (Haddad et al., 2013; Mohan et al., 2010; Tsou et al., 2012; van der Knaap et al., 2010; van der Knaap et al., 2005). Therefore, we sought novel interaction partners for non-stop (Figure 1A). To this end, an unbiased biochemical screen was designed to specifically identify protein complexes stably interacting with the distal, enzymatically active, SAGA DUBm (Figure 1B). Drosophila S2 cells were stably-transfected with pRmHa3-based inducible expression vectors to produce epitope-tagged Atxn7-2xFLAG-2xHA (Atxn7-FH), or non-stop-2xFLAG-2xHA (non-stop-FH) (Bunch et al., 1988; Cherbas et al., 2011; Guelman et al., 2006; Kusch et al., 2004; Mohan et al., 2014b; Suganuma et al., 2008). Cells stably transfected with empty vector served as negative control and Atxn7-FH cells served as positive control since Atxn7 has been previously characterized by purification, gel filtration, and mass spectrometry (Mohan et al., 2014b).

Protein complexes containing either non-stop or Atxn7 were purified from nuclear extracts via tandem purification of their epitope tags: FLAG, then HA (Suganuma et al., 2010). Isolated complexes were separated by size using Superose 6 gel filtration chromatography (Figure 1C) (Kusch et al., 2003). To identify fractions containing enzymatically active non-stop, the ubiquitin-AMC deubiquitinase activity assay was performed, in which fluorescent probe AMC is initially quenched by conjugation to ubiquitin but fluoresces upon release by deubiquitination, permitting an indirect measurement of the relative amount of deubiquitination in each sample (Figure 1C) (Köhler et al., 2010; Samara et al., 2010a).

In complexes purified through Atxn7, peak deubiquitinase activity was detected around 1.8MDa, consistent with SAGA complex and previous purification, fractionation, and mass spectrometry of Atxn7 (Kusch et al., 2003; Lee et al., 2011b; Mohan et al., 2014b). In non-stop purifications, however, deubiquitinase activity resolved into three major peaks. The major activity peak resolved about 1.8 MDa, along with SAGA, and was labeled “Group 1”. A secondary peak, “Group 2”, was resolved centering approximately 669 kDa, which was interpreted to be non-SAGA large multi-protein complexes. A final peak with the lowest enzymatic activity, centering about 75 kDa, was labeled “Group 3.” The DUBm, consisting of non-stop, Sgf11, and E(y)2 are predicted to have a molecular mass of 88 kDa, meaning this last peak was the DUBm interacting with very small proteins, if any.

Three fractions comprising the center of each peak were combined, and MudPIT mass spectrometry performed to identify the protein constituents of each (Washburn et al., 2001). Consistent with previous characterizations of SAGA, Group 1 contained SAGA complex subunits from each of the major (HAT/TAF/SPT/DUB) modules (Kusch et al., 2003; Lee et al., 2011b; Mohan et al., 2014b; Setiaputra et al., 2015). Previous fractionation demonstrated that Atxn7 is present in group 1 alone (Mohan et al., 2014b). Groups 2 and 3 contained the DUBm: non-stop, Sgf11, and e(y)2 – indicating the DUBm remained intact during purification and fractionation (Köhler et al., 2010; Lee et al., 2011b; Samara et al., 2010a). SAGA subunits characteristic of the larger complex, Nipped A (SPT module) and Ada2b (HAT module), were absent from groups 2 and 3 (Figure 1D). Histone H2A and H2B were detected in both groups 1 and 2, suggesting the DUBm was co-purifying with known substrates, and further confirming conditions were suitable for preservation and identification of endogenous interactions (Figure 2A) (Henry et al., 2003; Zhao et al., 2008). Furthermore, non-stop distributed normalized spectral abundance (dNSAF) was not over-represented relative to Sgf11 and e(y)2, showing non-stop bait protein was not expressed beyond physiological levels (Figure 2A) (Zhang et al., 2010).

Non-stop co-purifies with Arp2/3 and WRC complexes

MudPit proteomics provides a dNSAF factor which acts as a reporter for relative protein amount within a sample (Washburn et al., 2001). Notably, within Group 2, Arp2/3 complex (all subunits) and WRC subunits SCAR, Hem, and Sra-1 were represented in high ratio to DUBm members, as determined by dNSAF (Figure 2A) (Chen et al., 2010; Pollard and Beltzner, 2002).

WRC complex activates Arp2/3 to promote actin branching, which is important for a range of cellular activities including cell migration, cell adhesion, exocytosis, endocytosis, maintenance of nuclear shape, and phagocytosis (Alekhina et al., 2017; Navarro-Lerida et al., 2015; Takenawa and Miki, 2001; Verboon et al., 2015; Vishavkarma et al., 2014; Zallen et al., 2002). Non-stop and Atxn7-containing complexes were purified from nuclear extracts, where their function in gene regulation has been best characterized. WRC and Arp2/3 function in the nucleus is more enigmatic. Although Arp2/3 and WRC have demonstrated nuclear functions, their roles in actin branching in the cytoplasm are better understood (Miyamoto et al., 2013; Navarro-Lerida et al., 2015; Rawe et al., 2004; Verboon et al., 2015; Yoo et al., 2007). SAGA, WRC, and Arp2/3 complexes are all critical for proper central nervous system function, making the regulatory intersection for these complexes intriguing for further study (Chou and Wang, 2016; Dumpich et al., 2015; Irie and Yamaguchi, 2004; Kessels et al., 2011; Meyer and Feldman, 2002; Zallen et al., 2002).

In Drosophila, SCAR is particularly important for cytoplasmic organization in the blastoderm, for egg chamber structure during oogenesis, axon development in the central nervous system, and adult eye morphology (Zallen et al., 2002). To further characterize the relationship between non-stop, Atxn7 and WRC, we turned to the BG3 cell line (ML-DmBG3-c2, RRID:CVCL_Z728). These cells were derived from the Drosophila third instar larval central nervous system. Biochemical and RNAseq profiling of these cells indicate they express genes associated with the central nervous system, express neurotransmitters, are specifically detected with reagents used to probe for neuronal cells (such as HRP), and readily form neuroblasts. Their morphology is similar to that of mammalian astrocytes, which are used widely as a model for neurodegenerative disease. (Cherbas et al., 2011; Ui-Tei et al., 1994; Ui-Tei et al., 1995; Ui et al., 1994).

To verify interaction between non-stop and WRC, BG3 cells were transiently transfected with either non-stop-FH or SCAR-2xFLAG-2xHA (SCAR-FH) and immunoprecipitated with anti-FLAG resin. An anti-HA antibody was used to verify pull down of the tagged protein. A previously verified anti-SCAR antibody confirmed the presence of SCAR in non-stop-FH immunoprecipitate (Figure 2B) (Cetera et al., 2014; Evelyn Rodriguez-Mesa, 2012; Tran et al., 2015; Verboon and Parkhurst, 2015; Verboon et al., 2015). Reciprocal immunoprecipitation of SCAR-FH utilizing an anti-FLAG resin followed by immunoblotting for non-stop using a previously characterized anti-non-stop antibody confirmed endogenous non-stop associated with SCAR-FH (Figure 2C) (Mohan et al., 2014b).

To visualize the scope of non-stop and WRC colocalization, indirect immunofluorescence was used to localize endogenous SCAR and non-stop in BG3 cells. In these stationary cells, SCAR localized throughout the cytoplasm, reaching into long bimodal processes extending from the cell body (Figure 2D). Non-stop localized similarly to SCAR, but also within nuclei. When we examined the spatial relationship between non-stop and F-actin, using phalloidin, we observed non-stop overlapping with portions of phalloidin (Figure 2E) (Cooper, 1987).

Atxn7 and non-stop coordinate SCAR protein levels

The interaction of the DUBm with SAGA is regulated by Atxn7, meaning the amount of non-stop available for interaction with SCAR increases upon loss of Atxn7 (Mohan et al., 2014b). If non-stop was acting as a SCAR deubiquitinase to counter proteolytic degradation, then reducing non-stop would lead to less SCAR protein. Conversely, we would expect increased SCAR protein upon loss of Atxn7. To test these hypotheses, we used RNAi to knock down non-stop or Atxn7 transcripts in cell culture and observed SCAR protein levels by immunoblotting. BG3 cells were soaked in dsRNA targeting LacZ (negative control), non-stop, or Atxn7. After five days, denaturing whole cell protein extracts were prepared from these cells and immunoblotted to detect SCAR. Ponceau S total protein stain was used as loading control to verify analysis of equal amounts of protein (Lee et al., 2016; Romero-Calvo et al., 2010). Protein extracts from non-stop knockdown cells consistently showed about 70% decrease in SCAR protein levels relative to LacZ control knock-down. Consistent with a model in which Atxn7 restrains non-stop deubiquitinase activity, cells treated with Atxn7-targeting RNAs showed 2.5-fold increase in SCAR protein (Figure 3A). We verified these results by immunoblotting whole cell extracts prepared from the brains of 3rd instar larvae bearing homozygous mutations for *non-stop (not^{02069})*, a loss of function allele (Poeck et al., 2001) or *Atxn7* (*Ataxin7$^{[KG02020]}$*), a loss of function allele (Mohan et al., 2014b). Larval brain extracts showed about 75% decrease in SCAR protein levels in *non-stop* mutants (Figure 3B). In *Atxn7* mutant extracts, SCAR was increased 2.5-fold (Figure 3B).

Considering that SAGA is a known chromatin modifying complex best characterized for its role in gene regulation. We examined whether non-stop influences *SCAR* gene expression. In genome wide analysis of glial nuclei isolated from mutant larvae, *SCAR* transcript was significantly down regulated by one fold in non-stop deficient glia, but not in *Sgf11* deficient glia (Ma et al., 2016). Since Sgf11 is required for non-stop enzymatic activity, it is not clear what mechanism links *non-stop* loss to reduction in *SCAR* gene expression. To confirm the

relationship between non-stop and *SCAR* gene expression, we used qRT-PCR to measure *SCAR* transcript levels in BG3 cells knocked-down for *non-stop*. We found a similar one half decrease in *SCAR* transcript levels (Figure 3C). However, examination of *Atxn7* knockdown showed no decrease in *SCAR* transcript levels (Figure 3C). These results suggest *non-stop* loss leads to modest decreases in *SCAR* transcripts, but *SCAR* gene expression is independent of *Atxn7* or *Sgf11*, suggesting this gene is not SAGA-dependent or dependent on non-stop enzymatic activity. To determine the consequences of reducing *SCAR* transcripts by half on the level of SCAR protein, we examined *SCAR* heterozygous mutant larval brains ($SCAR^{[Delta37]}$/+). qRT-PCR analysis showed heterozygous *SCAR* brains produced 40% less *SCAR* transcript than wild-type brains (Figure 3D). However, heterozygous *SCAR* mutant and wild-type brains showed similar amounts of protein, demonstrating this amount of transcript is sufficient for full production of SCAR protein (Figure 3E). Since *non-stop* mutants showed a similarly modest decrease in *SCAR* gene expression but a contrasting drastic decrease in protein levels, and considering the interaction of DUBm and WRC proteins, we tested the possibility that non-stop counters SCAR protein degradation post-translationally.

Purification and mass spectrometry identified WRC members SCAR, HEM, and SRA-1, as interaction partners of the independent DUBm (Figure 2A). In Drosophila, HEM, SRA-1, and Abi recruit an unidentified deubiquitinase to balance SCAR regulation through a constant ubiquitination-proteasomal degradation mechanism facilitating rapid changes in SCAR protein amount and localization (Kunda et al., 2003). In mammals, the USP7 deubiquitinase acts as a molecular rheostat controlling proteasomal degradation of WASH (Hao et al.). To determine whether non-stop similarly regulates SCAR entry into a proteasomal degradation pathway in Drosophila we utilized *ex vivo* culture of 3rd instar larval brains to permit pharmacological inhibition of the proteasome (Rabinovich et al., 2015; Ranjini Prithviraj, 2012). Wandering 3rd instar larval brains were isolated from non-stop homozygous mutant larvae and cultured for 24 hours in the presence of MG132 proteasome inhibitor. Treating *non-stop* brains with MG132 rescued SCAR protein amounts to levels found in wild type brains (Figure 3F). Rescue of SCAR protein by proteasome inhibition suggests non-stop counteracts SCAR protein entry into a proteasomal degradation pathway.

Non-stop regulates SCAR protein levels and localization

To examine whether increasing non-stop led to increased SCAR, we expressed recombinant non-stop in BG3 cells and utilized indirect immunofluorescence to observe the amount and location of endogenous SCAR protein. Upon expression of non-stop-FH in BG3

cells, endogenous SCAR protein levels increased 5-fold compared with mock transfected cells (Figure 4A). Utilizing anti-HA immunofluorescence to observe recombinant non-stop, three distinct subcellular localization patterns were apparent: nuclear, cytoplasmic, and evenly distributed between nucleus and cytoplasm (Figure 4A). Increased SCAR protein co-compartmentalized with non-stop, even within the nucleus, where SCAR function is more enigmatic (Figure 4A). To quantify co-compartmentalization of SCAR and non-stop, we calculated the nuclear to cytoplasmic ratios of non-stop-FH and endogenous SCAR by dividing immunofluorescence intensity within each nuclei by that of the corresponding cytoplasm. This was plotted as the ratio nuclear:cytoplasmic SCAR on the Y axis and the ratio nuclear:cytoplasmic non-stop on the X axis. As the amount of non-stop in the nucleus increased, so did the amount of SCAR in the nucleus, showing that non-stop was driving SCAR localization (R^2=0.8) (Figure 4A).

SCAR functions, within the WRC, to activate Arp2/3 and facilitate branching of F-actin filaments (Kurisu and Takenawa, 2009). With correct spatiotemporal regulation of these actin-branching complexes, cells are able to establish appropriate shape and size through the extension of actin-based protrusions (Blanchoin et al., 2014). If non-stop overexpression were disrupting SCAR function through augmenting and mislocalizing SCAR protein, we expected to observe changes in cell shape and ability to form protrusions. When we used phalloidin to observe F-actin in cells overexpressing non-stop, a dramatic change in cell morphology was observed. Cells displayed fewer projections and covered less total area (Figure 4B). This was especially pronounced in cells expressing non-stop in the cytoplasm or both nucleus and cytoplasm. Overexpression of SCAR alone led to similar reductions in cell area and number of projections observed. Increased non-stop signal associated closely with increased phalloidin signal.

Non-stop bears multiple, conserved, WRC interacting receptor sequence (WIRS) motifs

We sought the basis for interaction between the SAGA DUBm, Arp2/3, and WRC. Some SCAR-interacting proteins bear a WRC interacting receptor sequences: (WIRS) motif (Chen et al., 2014). Primary sequence analysis of DUBm subunits revealed four WIRS-conforming sequences on non-stop and the mammalian orthologue USP22. These were conserved in number and relative location (Figure 5A). With the exception of non-stop, none of the DUBm components bore conserved WIRS motifs. Therefore, we focused on non-stop WIRS motifs. These were numbered from 0 to 3, with WIRS1, 2, and 3 conserved in location between Drosophila and mammalian non-stop (Figure 5A). Analysis of the yeast orthologue of non-stop

(UBP8) did not reveal a WIRS-like motif, but the Atxn7 orthologue Sgf73 did. In yeast, the DUBm is also be found separate from SAGA, although not without Sgf73 (Lim et al., 2013).

To determine if non-stop WIRS sequences are relevant for functional interaction with SCAR, we produced a series of phenylalanine to alanine point mutants in the putative WIRS domains (WIRS F-A) and expressed them in BG3 cells. As above, we measured the ability of non-stop WIRS mutants to increase the levels of endogenous SCAR protein, to change cell area, and to change the number of protrusions per cell. Immunofluorescence was used to detect the HA epitope on exogenously expressed non-stop and an antibody toward endogenous SCAR was used to observe SCAR protein levels. We analyzed cells expressing moderate amounts of non-stop as judged by the spectrum of fluorescence intensity to avoid analyzing cells with either too little or too much exogenous non-stop relative to endogenous protein. We calculated the ratio of HA fluorescence to SCAR fluorescence in each mutant and compared this to wild type non-stop (Figure 5B). In each case, the mutant non-stop produced less SCAR protein than wild type, suggesting that these motifs are indeed important for non-stop mediated increases in SCAR protein levels (Figure 5B). Mutant non-stop was also less potent for decreasing cell area and decreasing the number of cell protrusions (Figure 5C).

Discussion

Purification of Atxn7-containing complexes indicated that Atxn7 functions predominantly as a member of SAGA (Mohan et al., 2014b). In yeast, the Atxn7 orthologue, Sgf73, can be separated from SAGA along with the deubiquitinase module by the proteasome regulatory particle (Lim et al., 2013). Without Sgf73, the yeast deubiquitinase module is inactive (Samara et al., 2010b). In higher eukaryotes Atxn7 increases, but is not necessary for non-stop/USP22 enzymatic activity in vitro (Lan et al., 2015; Mohan et al., 2014b). In Drosophila, loss of Atxn7 leads to a non-stop overactivity phenotype, with reduced levels of ubiquitinated H2B observed (Mohan et al., 2014b). Purification of non-stop revealed the active SAGA DUBm associates, separate from SAGA, with multi-protein complexes including WRC and Arp2/3 complexes. SCAR was previously described to be regulated by a constant ubiquitination/deubiquitination mechanism (Kunda et al., 2003). We found increased SCAR protein levels upon knockdown of Atxn7 and decreased SCAR protein levels upon knockdown of non-stop. We found that that decreases in SCAR protein levels in the absence of non-stop required a functional proteasome.

When we overexpressed non-stop, we found an increase in SCAR protein levels. Increases in SCAR protein colocalized to subcellular compartments where non-stop protein levels increased. Nuclear Arp2/3 and WRC have been linked to nuclear reprogramming during

early development, immune system function, and general regulation of gene expression (Miyamoto et al., 2013; Taylor et al., 2010; Yoo et al., 2007). Distortions of nuclear shape have been shown to alter chromatin domain location within the nucleus, resulting in changes in gene expression (Evelyn Rodriguez-Mesa, 2012; Navarro-Lerida et al., 2015).

When we examined the basis for this unexpected regulatory mechanism, we uncovered a series of WIRS motifs (Chen et al., 2014) conserved in number and distribution between flies and mammals. These sequences functionally modulate non-stop ability to increase SCAR protein levels. Point mutants of each WIRS resulted in less SCAR protein per increase in non-stop protein.

Overall, these findings suggest that SAGA maintains a pool of non-stop that can be made available to act distally from the larger SAGA complex to modulate SCAR protein levels (Figure 6). Already, it has been shown that in yeast, the proteasome regulatory particle can mediate removal of the DUBm from SAGA (Lim et al., 2013). In higher eukaryotes, caspase 7 cleavage has been shown to act on Atxn7 at residues which would be expected to release the DUBm, although this has not been explicitly shown (Young et al., 2007). The mechanisms orchestrating entry and exit of the DUBm from SAGA remain to be explored.

Figure Legends

Figure 1. Atxn7 co-purifies with SAGA, but non-stop co-purifies with SAGA and additional multi-protein complexes. (A) Schematic of the working model that the deubiquitinase module can function independent of SAGA. Non-stop is anchored to the SAGA complex by Atxn7. Non-stop can also be found outside of SAGA during wild type conditions and interacts with unknown proteins. (B) Scheme to identify non-stop interactors. (C) Ubiquitin-AMC assay measuring deubiquitinase activity. Fluorescence increases as deubiquitination increases. The top panel is the measure of activity when Atxn7 is used as bait. The bottom panel is the measure of activity when non-stop is bait. (D) Fractions from non-stop containing complexes were split into three groups and constituent proteins identified by mass spectrometry. dNSAF values for SAGA complex member in group 1 (blue) vs group 2 (red) reveal that while components of the deubiquitinase module (non-stop and Sgf11) are found in both group 1 and group 2 other components of SAGA (Ada2b and Nipped A) are specifically found in group 1 and not group 2.

Figure 2. The Arp2/3 and WRC complexes interact with the SAGA deubiquitinase module. (A) Mass spectrometry data from Group 2 fractions show the Arp2/3 and WRC complexes interact stably with non-stop. Total represents the entire amount of the protein in the sample. “Group 2” fraction is the amount of the protein represented in group. The negative control is a vector only sample. (B) BG3 cells were either treated with transfection reagent and no plasmid (Control) or transfected with non-stop-2xFLAG-2xHA (non-stop-FH). Proteins were immunoprecipitated using FLAG beads. The extracts were immunoblotted for the presence of SCAR. The extracts were immunoblotted for HA to verify presence of non-stop-FH. NS marks a non-specific band. (C) BG3 cells were either treated with transfection reagent and no plasmid (Control) or transfected with SCAR-2xFLAG-2xHA (SCAR-FH). Proteins were immunoprecipitated using FLAG beads. The extracts were immunoblotted for the presence of non-stop. The extracts were immunoblotted for HA to verify immunoprecipitation of SCAR-FH. (D) Immunofluorescence of SCAR and non-stop in BG3 cells. Cells were immunostained with anti-non-stop (magenta), anti-SCAR (yellow), and DAPI (white). Scale bar is 10 µM. Inset is enlarged to the right. (E) Representative images of BG3 cells immunostained with anti-non-stop (magenta), phalloidin (yellow), and DAPI (white). Scale bar is 10 µM. Inset is enlarged to the right.

Figure 3. non-stop regulates SCAR protein levels. (A) Immunoblot for SCAR protein levels in BG3 cells treated with dsRNA targeting either LacZ, Atxn7, or non-stop (not). Ponceau staining for total protein levels controls for equal loading of extracts. Three independent samples were immunoblotted and band intensity was measured. All values were normalized to ponceau and numbers are set relative to the LacZ control. (B) Western blots for SCAR protein in larval brains dissected from Oregon R (WT), *non-stop*^{02069} *(not*), and *Ataxin7*$^{[KG02020]}$ (*Atxn7*) third instar larva. Ponceau total protein loading control is shown. SCAR band intensity measured from three experiments and average intensity is shown. All lanes are normalized to total protein levels (Ponceau) and set relative to OregonR (WT). (C) Relative quantitation of SCAR transcript levels in BG3 cells treated with dsRNA targeting either LacZ, Atxn7, or non-stop (not). Transcript levels from LacZ treated cells were set to one and transcripts from non-stop and Atxn7 treated cells are relative to LacZ treated cells. (D) Relative quantitation of SCAR transcript levels in larval brains dissected from OregonR (WT) or *SCAR*$^{[Delta37]}$/cyo-gfp (*SCAR*/+). SCAR transcript levels are set relative to WT. (E) Immunoblot for SCAR protein in larval brains dissected from

OregonR (WT) or *SCAR*$^{[Delta37]}$/cyo-gfp (*SCAR*/+). Total protein levels measured by Ponceau were used as a loading control. Band intensity of three extracts was measured and averaged. Protein levels were set relative to OregonR (WT) and normalized to Ponceau. (F) Oregon R (WT) and non-stop (not) brains were dissected from third instar larva and cultured. Half of the brains from each genotype were treated with 50 µm MG132 (MG132+) the other half of the brains from each genotype remained untreated (MG132-) for 24 hours of culturing. Representative immunoblot for SCAR on protein extracts from cultured larval brains and the Ponceau loading control. Band intensity of SCAR was measured from three independent samples and averaged. All values were normalized to Ponceau and numbers are set relative to the untreated WT samples. No MG132 treatment is to the left and treatment with MG132 is to the right.

Figure 4. Overexpression of non-stop increases SCAR levels and changes cellular morphology. (A) BG3 cells were either treated with transfection reagent and no plasmid (Control) or transfected with non-stop-FH. Cells were fixed and immunostained with anti-HA (magenta), anti-SCAR (yellow), and DAPI (white). Scale bar is 10 µM. Circles outline DAPI (inner circle) and the edge of the cell (outer circles). Three categories of HA (non-stop-FH) expression are shown: non-stop nuclear, non-stop cytoplasmic, and non-stop nuclear and cytoplasmic. Total SCAR intensity was measured in HA positive cells (non-stop-FH) and mock transfected cells (Control). Intensities are set relative to control cells. SCAR intensity was measured in the nucleus (as determined by DAPI) and in the cytoplasm. A ratio of nuclear SCAR intensity divided by cytoplasmic SCAR intensity was calculated. HA intensity was measured in the nucleus and in the cytoplasm. A ratio of nuclear HA intensity to cytoplasmic HA intensity was calculated. The HA ratio was plotted on the X axis and the SCAR ratio was plotted on the Y axis. A trend line was added and an R^2 was calculated. (B) Immunostained BG3 cells that were either treated with transfection reagent and no-plasmid (Control), non-stop-FH, or SCAR-FH. Cells were stained with anti-HA (magenta), phalloidin (yellow), and DAPI (white). Scale bar is 10 µM. Cell area was measured and total number of cellular projections was counted in HA positive cells (non-stop-FH or SCAR-FH) and compared to mock transfected (Control) cells. Cells expressing non-stop-FH were split into three categories of HA (non-stop-FH) expression: non-stop nuclear, non-stop cytoplasmic, and non-stop nuclear and cytoplasmic. T-tests were used to compare the samples and p-values are shown.

Figure 5. non-stop contains conserved WIRS motifs (A) Alignment of non-stop protein sequences reveals a conserved distribution of WIRS motifs between higher eukaryotes. (B) BG3 cells were transfected with either the wild type version of non-stop-FH (WT) or non-stop-FH harboring a point mutation in one of the four putative WIRS motifs (W0-W3). Cells were fixed and immunostained with anti-HA (magenta), anti-SCAR (yellow), and DAPI (white). Scale bar is 10 µM. Total fluorescence intensity of SCAR and HA was measured in HA containing cells. Box plots show the SCAR intensity divided by the intensity of HA for cells expressing either the wild type version of non-stop-FH (WT) or non-stop-FH harboring a point mutation in one of the four putative WIRS motifs (W0-W3). T-tests were used to compare samples and p-values are shown. (C) BG3 cells transfectected with either the wild-type version of non-stop-FH (WT) or non-stop-FH harboring a point mutation in one of the four putative WIRS motifs (W0-W3) were immunostained for HA (magenta) and phalloidin (yellow). Scale bar is 10 µm. Arrows point to

localized accumulation of non-stop WIRS mutant protein, which coincide with aberrant actin protrusions commonly observed upon WRC or Arp2/3 loss of function. Cell area and number of projections protruding from cells was determined for HA positive (non-stop overexpressing) cells. T-tests were used to compare the samples and p-values are shown.

Figure 6. non-stop deubiquitinates SCAR. Model showing non-stop interacts with the WRC in an Atxn7-dependent manner, where it counteracts ubiquitination and subsequent protein degradation of WRC subunit SCAR. Loss of Atxn7 leads to increased availability of non-stop for interaction with the WRC.

Methods

Cell culture

BG3 cells were grown in Schneider's media supplemented with 10% fetal bovine serum and 1:10,000 insulin. S2 cells were maintained in Schneider's media supplemented with 10% fetal bovine serum and 1% pen-strep.

Transfection

BG3 cells were plated at 0.5 x10^6 cells/ml, forty eight hours later they were transfected using Lipofectamine 3000 (ThermoFisher catalog number: L3000015) following the manufacturer's directions. The Lipofectamine 3000 was used at 1 µl per µg of DNA and p3000 reagent was used at 2 µl per µg of DNA to be transfected. To induce expression of proteins from plasmids containing a metalothienine promoter 250 µm of $CuSO_4$ was added to the media. For transfections taking place in 6 well dishes 1 µg of DNA was used per well and 15 µg of DNA was used per 15 cm dish. Proteins were given 2 days of expression before the samples were used.

Plasmids

Scar (Berkley Expression Clone Collection FMO14142) (Yu et al., 2011)
Prmha3-non-stop-2XFlag-2XHA (ubiquitin-specific protease nonstop [Drosophila melanogaster] Sequence ID: AAD53181.1) (Poeck et al., 2001)
Prmha3-non-stop-2XFlag-2XHA-0FA, Prmha3-non-stop-2XFlag-2XHA-1FA, Prmha3-non-stop-2XFlag-2XHA-2FA, Prmha3-non-stop-2XFlag-2XHA-3FA, and Prmha3-non-stop-2XFlag-2XHA-4FA were created using quick change mutagenesis using Prmha3-non-stop-2XFlag-2XHA as a template following the manufacturer's directions.
Primer list for quickchange mutagenisis:
WIRS0 phenylalenine to alenine F: GCAGTGGCCGAAGCGCCGGCAGGGGAACGGAACGGTGGGC
WIRS0 phenylalenine to alenine R: CCGTTCCCCTGCCGGCGCTTCGGCCACTGCTGCTGCTGC
WIRS1 phenylalenine to alenine F: CAGCTACGATACAGCCCGGGTCATCGACGCCTACTTCGCTGCTTGCG
WIRS1 phenylalenine to alenine R: GGCGTCGATGACCCGGGCTGTATCGTAGCTGTGCTCCTTCACATAGC
WIRS2 phenylalenine to alenine F: GTCTCTTCCAGGAGGCCTATTCCGGCTCCCGTTCGCCGCTGTCGC
WIRS2 phenylalenine to alenine R: GGAGCCGGAATAGGCCTCCTGGAAGAGACGTGACACTTCACAAACG
WIRS3 phenylalenine to alenine F: CCAGCGTGGTGTCGGCCCATTTGAAACGCTTCGAGCACTCAGCTCTG
WIRS3 phenylalenine to alenine R: CGAAGCGTTTCAAATGGGCCGACACCACGCTGGGCAGAGTGCGCAG
WIRS4 phenylalenine to alenine F: CGCAAGATCTCCTCGGCCATTCAATTCCCCGTGGAGTTCGACATG
WIRS4 phenylalenine to alenine R: CCACGGGGAATTGAATGGCCGAGGAGATCTTGCGATCGATCAGAGC

RNAi treatment of BG3 cells

Short dsRNA was produced by amplifying cDNA with primers that contained T7 promoter sequences on the ends. These PCR products were then used as a template for in vitro transcription using the Ampliscribe T7 high yield transcription kit (epicentre catalog number: AS3107) following the manufacturer's instructions. Transcription was allowed to continue for four hours. To make the RNA double stranded it was then heated at 65 °C for thirty minutes and cooled to room temperature. The RNA was then ethanol precipitated in order to clean it.

BG3 cells were plated at $2x10^6$ cells/ml in 6 well dishes. Cells were allowed to adhere (approximately four hours) then treated with 10 µg of dsRNA. The cells were harvested for western blot after being soaked for six days and after five days for RNA analysis.

RNAi

Atxn7 DRSC23138, Atxn7 DRSC35628, non-stop BKN21994, non-stop DRSC11378
dsRNA-LacZ-R: GCTAATACGACTCACTATAGGCCAAACATGACCARGATTACGCCAAGCT
dsRNA-LacZ-F: GCTAATACGACTCACTATAGGCCAAACGTCCCATTCGCCATTCAGGC

Immunofluorescence

Cells were plated directly onto coverslips in 6 well dishes and allowed to adhere. BG3 cells were fixed in 4% methanol free formaldehyde after two days of growth. Cells were washed in 1xPBS and then either stored in 1xPBS for up to one week or immediately stained. Coverslips were washed with 1xPBS containing 0.5% Triton X-100 four times for 10 minutes. Coverslips were blocked in 5% BSA and 0.2% TWEEN 20 diluted in 1xPBS for one hour at room temperature. They were then incubated in primary antibody diluted in blocking buffer overnight at 4 °C. The following day they were washed with 1xPBS containing 0.5% Triton X-100 four times for ten minutes. They were then incubated in secondary antibody diluted 1:1000 in blocking buffer for four hours at room temperature. Cells were then washed four times ten minutes at room temperature in 1xPBS containing 5% Triton X-100. Coverslips were dried and mounted in Vectashield containing DAPI (Vector Labs catalog number: H-1200).

A Zeiss LSM-5 Pascal upright microscope and LSM software was used for imaging. Cells were imaged with a 40X objective aperture number 1.30 oil or a 63X objective aperture number XXX and Z-stacks were acquired using LSM software with a slice every 1 µm. Brains were imaged with a 20X objective aperture number 0.45 air and Z stacks were taken with slices every 4 µm. All images were taken at room temperature. All settings remained the same within an experiment.

Antibodies

Mouse anti SCAR (DSHB P1C1-SCAR) was used at a dilution of 1:100. Rat anti HA (Roche catalog number: 11867423001) was used at a dilution of 1:1000. Guinea pig anti non-stop (Mohan et al., 2014b) was used at a dilution of 1:500. Goat anti Rat IGG -568 (Invitrogen Catalog number: A-11077) was used at a dilution of 1:1000. Goat anti Mouse IGG-488 (Invitrogen Catalog number: A-11001) was used at a dilution of 1:1000. Goat anti Guinea pig IGG- 488 (Invitrogen Catalog number: A11073) was used at a dilution of 1:1000. Phalloidin-488 (Invitrogen Catalog number: A12379) was used at a dilution of 1:20. Phalloidin-568 (Invitrogen Catalog number: A12380) was used at a dilution of 1:20.

Image analysis

Stacks were exported as TIFFs from the LSM software and analyzed in ImageJ. For analysis z projections were created by sum.

To analyze cell shape and phalloidin structures in BG3 cells the Phalloidin images were thresholded in ImageJ and used to create ROIs. The number of projections was counted by

hand. A t-test was used to test the significance between the mock transfected control and the non-stop-2xFlag-2 transfected cells lines in cellular shape and the number of projections.

To measure SCAR levels in BG3 and S2 cells ROIs were drawn by hand around the entirety of the scar staining and integrated density was measured for both HA and SCAR. For BG3 cells a second ROI was drawn around the nuclei and the scar intensity of the SCAR and HA was measured. Thresholding the original image and using image calculator subtracted background. A t-test was used to compare between treated and untreated cells.

Ex vivo culturing of third instar brains

Ex vivo culturing of larval brains was performed as described (Rabinovich et al., 2015; Ranjini Prithviraj, 2012). Third instar brains were dissected in 1xPBS and quickly placed into culture media (Schneider's insect media supplemented with 10% FBS, 1% pen/strp, 1:10,000 insulin, and 2 µg/ml ecdysone) in 24 well dish. The dish was wrapped in parafilm and incubated at 25 °C. After 6 hours of culturing the media was changed. The wells receiving MG132 then had 50 µM of MG132 added. Brains were collected for protein samples after 24 hours.

Protein Sample Preparation

All western blots using tissue culture cells were done from cells collected from a 6 well dish. The media was removed and 200 µl of 2xUREA sample buffer (50 mM Tris HCl pH 6.8, 1.6% SDS, 7% glycerol, 8M Urea, 4% β mercaptoethanol, 0.016% bromophenol blue) and 2 µl of 10 µg/ml benzonase was added to the dish. After the mixture was lysed they were boiled at 80 °C for five minutes.

Larval brains were dissected into 1xPBS. The PBS was removed and 2xUREA sample buffer was added in a 1:1 ratio and 10 units of Benzonase was added. The brains were homogenized by pipetting and boiled at 80 °C for five minutes.

Immunoprecipitation

Transfected cells were resuspended in Extraction Buffer (20 mM HEPES (pH7.5), 25% Glycerol, 420 mM NaCl, 1.5 mM $MgCl_2$, 0.2 mM EDTA, 1:100 ethidium bromide. 1% NP-40 was added and the cells were pipetted up and down until the solution was homogenous. They were placed on ice for one hour with agitation every 10-15 minutes. They were then centrifuged for 45 minutes at 4 °C at 4,500 x g. The supernatant was placed into a new tube and stored at – 80 °C for up to one week. Lysates were thawed and 36 µg of protein was removed for input and mixed with 2 x Urea sample buffer (50 mM Tris-HCl (pH 6.8), 1% SDS, 7% Glycerol, 8 M Urea, 4% beta-mercapto-ethanol, 0.016% Bromophenol blue) and boiled for five minutes at 80 °C. An equal volume of dignum buffer (10 mM HEPES (pH 7.5), 1.5 mM $MgCl_2$, 10 mM KCl) was added to the lysates in order to adjust the salt concentration to 210 mM NaCl. The entire volume was added to 15 µl of Mouse IGG agarose (Sigma Catalog number: A0919) that had been equilibrated in one volume extraction buffer plus one volume dignum. They were then rotated at 4 °C for one hour. After one hour they were centrifuged for one minute at 4 °C at 4,500 x g. The supernatant was then added to anti-FLAG M2 Affinity Gel (Sigma Catalog number: A2220) that had been equilibrated in one volume extraction buffer plus one volume dygnum. They were then rotated for one hour at 4 °C. After one hour they were centrifuged at 4,500 x g at 4 °C for thirty seconds. The supernatant was removed and the gel was washed five times in extraction buffer

plus dygnum. The resin was then resuspended in 40 µl 2XUREA sample buffer and boiled for five minutes at 80 °C.

Western Blot

Protein samples were run on either 6% polyacrylamide gel (ImmunoPreciptiaton) or on 8% polyacrylamide gels (all other samples) in 1X Laemli electrode buffer. Proteins were transferred to Amersham Hybond P 0.45 µM PVDF membrane (catalog number: 10600023) using the Trans-blot turbo transfer system from biorad. The semidry transfer took place in Bjerrum Schafer-Nielsen Buffer with SDS (48 mM Tris, 39 mM Glycine, 20% Methanol, 0.1% SDS) at 1 Amp 25 V for 20 minutes. Membranes were stained in Ponceau (0.2% Ponceau S, 2 % Acetic Acid) for twenty minutes at room temperature as a loading control. The membrane was then briefly washed in 1XPBS and imaged on a Chemidoc MP Imaging system. Membranes were then washed three times for five minutes to remove excess ponceau. Membranes were then blocked for one hour in 5% non-fat dried milk diluted in 0.05% Triton-X 100 in 1XPBS. The membrane was then briefly rinse and incubated in primary antibody diluted in 1% non-fat dried milk diluted in 0.05% Triton-X 100 for either one hour at room temperature or overnight at 4°C. The membrane was then washed four times for five minutes in 1% Triton-X 100 diluted in 1XPBS. The membrane was then incubated for one hour at room temperature in secondary antibody diluted 1:5000 in 1% non-fat dried milk diluted in 0.05% Triton-X 100. The membrane was then washed four times for five minutes in 1% Triton-X 100 diluted in 1xPBS. Bioworld ICL (catalog number: 20810000-1) was used to visualize the proteins following the manufacturer's instruction. The chemiluminescence was imaged on a Chemidoc MP Imaging system. Band intensities were measured on ImageLab software.

Antibodies

Mouse anti SCAR (DSHB P1C1-SCAR) was used at a dilution 1:500. Rat anti HA-HRP (Roche catalog number: 12013819001) was used at a dilution of 1:1000. Guinea Pig anti non-stop (Mohan et al., 2014b) was used at a dilution of 1:1000. All secondary anti-bodies were used at 1:5000: Goat anti Guinea Pig HRP (Jackson ImmunoResearch INC catalog number: 106-035-003) and Goat anti mouse HRP (Jackson ImmunoResearch INC catalog number: 106-035-003).

QPCR

RNA was extracted using the Invitrogen PureLink RNA mini kit (Fisher catalog number: 12 183 018A) following the manufacturer's instructions. The optional on column DNA digest was performed using the PureLink DNase set (Fisher Catalog number: 12185010). The high capacity cDNA reverse transcription kit (ThermoFisher catalog number: 4374966) was used to create cDNA using the manufacturer's protocol. 3 µl of cDNA created from 1 µg of RNA was used in downstream qPCR analysis. TaqMan gene expression assays were run following the manufacturer's directions. PCR was performed using the TaqMan Universal PCR Master Mix (ThermoFisher catalog number: 4364340). The reactions were run on an ABI 7500 Real-time PCR machine.

TaqMan assay IDs

RpL32 Dm02151827_g1, SCAR Dm01810606_g1, Not Dm01823071_g1, Atxn7 Dm01800874_g1

Fly Strains

SCAR [Delta37]: w[*]; SCAR[Delta37] P(ry[+t7.2]=neoFRT)40A/CyO, , P(w[+mC]=GAL4-twi.G)2.2, P(UAS-2xEGFP)AH2.2. Atxn7: y[1] w[67c23]; P(y[+mDint2] w[BR.E.BR]=SUPor-P)CG9866[KG02020]/CyO, P(w[+mC]=GAL4-twi.G)2.2, P(UAS-2xEGFP)AH2.2. non-stop: P(ry[+t7.2]=PZ)not[02069] ry[506]/TM3, P(w[+mC]=GAL4-twi.G)2.3, P(UAS-2xEGFP)AH2.3, Sb[1] Ser[1]. Wild type: Oregon-R

Acknowledgements

Jerry L. Workman and Susan M. Abmayr for advice and guidance. Jakob Waterborg for contributing plasticware reagents and small equipment. Boyko Atanassov and Stone (Bayou) Chen for critical reading of early draft manuscripts. University of Missouri Faculty Scholars training program. Funding agencies – School of Biological Science, UMKC; University of Missouri Research Board; UMKC SEARCH and UMKC SUROP scholars programs; NIGMS grant 5R35GM118068 to J. Workman.

Author contributions

Veronica J. Cloud – Formal analysis, Investigation, Methodology, Project Administration, Supervision, Validation, Visualization, Writing – review and editing
Ellie Momtahan – Investigation (Made flies)
Jarrid L. Jack – Investigation (western blots)
Edgardo Leiva – Investigation (immunostaining)
Sarah Rapp – Investigation (fly brain dissections)
Sara Miller – Investigation (fly brain dissections)
Lauren G. Shelton – Investigation (Cloned Non-stop plasmid)
Richard A Pierce – Resources (Equipment assembly and maintenance)
Ying Zhang – Investigation, Formal Analysis (MudPit)
Laurence Florens – Investigation (MudPit)
Michael P Washburn – Investigation (MudPit)
Ryan D Mohan – Conceptualization, Funding Acquisition, Investigation, Methodology, Project Administration, Supervision, Visualization, Writing – original draft

References

Alekhina, O., E. Burstein, and D.D. Billadeau. 2017. Cellular functions of WASP family proteins at a glance. *J Cell Sci*. 130:2235-2241.

Atanassov, B.S., and S.Y. Dent. 2011. USP22 regulates cell proliferation by deubiquitinating the transcriptional regulator FBP1. *EMBO Rep*. 12:924-930.

Atanassov, B.S., Y.A. Evrard, A.S. Multani, Z. Zhang, L. Tora, D. Devys, S. Chang, and S.Y. Dent. 2009. Gcn5 and SAGA regulate shelterin protein turnover and telomere maintenance. *Mol Cell*. 35:352-364.

Blanchoin, L., R. Boujemaa-Paterski, C. Sykes, and J. Plastino. 2014. Actin dynamics, architecture, and mechanics in cell motility. *Physiological reviews*. 94:235-263.

Bonnet, J., C.-Y. Wang, T. Baptista, S.D. Vincent, W.-C. Hsiao, M. Stierle, C.-F. Kao, L. Tora, and D. Devys. 2014. The SAGA coactivator complex acts on the whole transcribed genome and is required for RNA polymerase II transcription. *Genes Dev*. 28:1999-2012.

Bunch, T.A., Y. Grinblat, and L.S. Goldstein. 1988. Characterization and use of the Drosophila metallothionein promoter in cultured Drosophila melanogaster cells. *Nucleic Acids Res*. 16:1043-1061.

Campello, L., J. Esteve-Rudd, N. Cuenca, and J. Martin-Nieto. 2013a. The ubiquitin-proteasome system in retinal health and disease. *Molecular neurobiology*. 47:790-810.

Campello, L., J. Esteve-Rudd, N. Cuenca, and J. Martín-Nieto. 2013b. The Ubiquitin–Proteasome System in Retinal Health and Disease. *Molecular neurobiology*. 47:790-810.

Cetera, M., G.R. Ramirez-San Juan, P.W. Oakes, L. Lewellyn, M.J. Fairchild, G. Tanentzapf, M.L. Gardel, and S. Horne-Badovinac. 2014. Epithelial rotation promotes the global alignment of contractile actin bundles during Drosophila egg chamber elongation. *Nat Commun*. 5:5511.

Chen, B., Z. Chen, K. Brinkmann, C.W. Pak, Y. Liao, S. Shi, L. Henry, N.V. Grishin, S. Bogdan, and M.K. Rosen. 2014. The WAVE Regulatory Complex Links Diverse Receptors to the Actin Cytoskeleton. *Cell*. 156:195-207.

Chen, Z., D. Borek, S.B. Padrick, T.S. Gomez, Z. Metlagel, A.M. Ismail, J. Umetani, D.D. Billadeau, Z. Otwinowski, and M.K. Rosen. 2010. Structure and control of the actin regulatory WAVE complex. *Nature*. 468:533-538.

Cherbas, L., A. Willingham, D. Zhang, L. Yang, Y. Zou, B.D. Eads, J.W. Carlson, J.M. Landolin, P. Kapranov, J. Dumais, A. Samsonova, J.H. Choi, J. Roberts, C.A. Davis, H. Tang, M.J. van Baren, S. Ghosh, A. Dobin, K. Bell, W. Lin, L. Langton, M.O. Duff, A.E. Tenney, C. Zaleski, M.R. Brent, R.A. Hoskins, T.C. Kaufman, J. Andrews, B.R. Graveley, N. Perrimon, S.E. Celniker, T.R. Gingeras, and P. Cherbas. 2011. The transcriptional diversity of 25 Drosophila cell lines. *Genome Res*. 21:301-314.

Chou, F.S., and P.S. Wang. 2016. The Arp2/3 complex is essential at multiple stages of neural development. *Neurogenesis (Austin, Tex.)*. 3:e1261653.

Cooper, J.A. 1987. Effects of cytochalasin and phalloidin on actin. *J Cell Biol*. 105:1473-1478.

David, G., N. Abbas, G. Stevanin, A. Dürr, G. Yvert, G. Cancel, C. Weber, G. Imbert, F. Saudou, E. Antoniou, H. Drabkin, R. Gemmill, P. Giunti, A. Benomar, N. Wood, M. Ruberg, Y. Agid, J.-L. Mandel, and A. Brice. 1997. Cloning of the SCA7 gene reveals a highly unstable CAG repeat expansion. *Nat Genet*. 17:65.

Dumpich, M., H.G. Mannherz, and C. Theiss. 2015. VEGF Signaling Regulates Cofilin and the Arp2/3-complex within the Axonal Growth Cone. *Current neurovascular research*. 12:293-307.

Evelyn Rodriguez-Mesa, M.T.A.-B., Alicia E. Rosales-Nieves, and Susan M. Parkhurst. 2012. Developmental Expression of Drosophila Wiskott-Aldrich Syndrome family proteins. *Developmental Dynamics*. 241:608-626.

Furrer, S.A., M.S. Mohanachandran, S.M. Waldherr, C. Chang, V.A. Damian, B.L. Sopher, G.A. Garden, and A.R. La Spada. 2011. SCA7 cerebellar disease requires the coordinated action of mutant

ataxin-7 in neurons and glia, and displays non-cell autonomous Bergmann glia degeneration. *The Journal of Neuroscience*. 31:16269-16278.

Garden, G. 1993. Spinocerebellar Ataxia Type 7. *In* GeneReviews((R)). M.P. Adam, H.H. Ardinger, R.A. Pagon, S.E. Wallace, L.J.H. Bean, K. Stephens, and A. Amemiya, editors. University of Washington, Seattle

University of Washington, Seattle. GeneReviews is a registered trademark of the University of Washington, Seattle. All rights reserved., Seattle (WA).

Giunti, P., G. Stevanin, P.F. Worth, G. David, A. Brice, and N.W. Wood. 1999. Molecular and Clinical Study of 18 Families with ADCA Type II: Evidence for Genetic Heterogeneity and De Novo Mutation. *The American Journal of Human Genetics*. 64:1594-1603.

Glinsky, G.V., O. Berezovska, and A.B. Glinskii. 2005. Microarray analysis identifies a death-from-cancer signature predicting therapy failure in patients with multiple types of cancer. *The Journal of clinical investigation*. 115:1503-1521.

Guelman, S., T. Suganuma, L. Florens, S.K. Swanson, C.L. Kiesecker, T. Kusch, S. Anderson, J.R. Yates, 3rd, M.P. Washburn, S.M. Abmayr, and J.L. Workman. 2006. Host cell factor and an uncharacterized SANT domain protein are stable components of ATAC, a novel dAda2A/dGcn5-containing histone acetyltransferase complex in Drosophila. *Mol Cell Biol*. 26:871-882.

Haddad, Dominik M., S. Vilain, M. Vos, G. Esposito, S. Matta, Vera M. Kalscheuer, K. Craessaerts, M. Leyssen, Rafaella M.P. Nascimento, Angela M. Vianna-Morgante, B. De Strooper, H. Van Esch, Vanessa A. Morais, and P. Verstreken. 2013. Mutations in the Intellectual Disability Gene Ube2a Cause Neuronal Dysfunction and Impair Parkin-Dependent Mitophagy. *Molecular Cell*. 50:831-843.

Hao, Y.-H., Michael D. Fountain, Jr., K. Fon Tacer, F. Xia, W. Bi, S.-Hae L. Kang, A. Patel, Jill A. Rosenfeld, C. Le Caignec, B. Isidor, Ian D. Krantz, Sarah E. Noon, Jean P. Pfotenhauer, Thomas M. Morgan, R. Moran, Robert C. Pedersen, Margarita S. Saenz, Christian P. Schaaf, and Patrick R. Potts. USP7 Acts as a Molecular Rheostat to Promote WASH-Dependent Endosomal Protein Recycling and Is Mutated in a Human Neurodevelopmental Disorder. *Molecular Cell*. 59:956-969.

Henry, K.W., A. Wyce, W.-S. Lo, L.J. Duggan, N.C.T. Emre, C.-F. Kao, L. Pillus, A. Shilatifard, M.A. Osley, and S.L. Berger. 2003. Transcriptional activation via sequential histone H2B ubiquitylation and deubiquitylation, mediated by SAGA-associated Ubp8. *Genes Dev*. 17:2648-2663.

Irie, F., and Y. Yamaguchi. 2004. EPHB receptor signaling in dendritic spine development. *Frontiers in bioscience : a journal and virtual library*. 9:1365-1373.

Kessels, M.M., L. Schwintzer, D. Schlobinski, and B. Qualmann. 2011. Controlling actin cytoskeletal organization and dynamics during neuronal morphogenesis. *European journal of cell biology*. 90:926-933.

Köhler, A., E. Zimmerman, M. Schneider, E. Hurt, and N. Zheng. 2010. Structural Basis for Assembly and Activation of the Heterotetrameric SAGA Histone H2B Deubiquitinase Module. *Cell*. 141:606-617.

Kunda, P., G. Craig, V. Dominguez, and B. Baum. 2003. Abi, Sra1, and Kette control the stability and localization of SCAR/WAVE to regulate the formation of actin-based protrusions. *Current biology : CB*. 13:1867-1875.

Kurisu, S., and T. Takenawa. 2009. The WASP and WAVE family proteins. *Genome Biol*. 10:226.

Kusch, T., L. Florens, W.H. Macdonald, S.K. Swanson, R.L. Glaser, J.R. Yates, 3rd, S.M. Abmayr, M.P. Washburn, and J.L. Workman. 2004. Acetylation by Tip60 is required for selective histone variant exchange at DNA lesions. *Science*. 306:2084-2087.

Kusch, T., S. Guelman, S.M. Abmayr, and J.L. Workman. 2003. Two Drosophila Ada2 homologues function in different multiprotein complexes. *Mol Cell Biol*. 23:3305-3319.

Lan, X., E. Koutelou, A.C. Schibler, Y.C. Chen, P.A. Grant, and S.Y. Dent. 2015. Poly(Q) Expansions in ATXN7 Affect Solubility but Not Activity of the SAGA Deubiquitinating Module. *Mol Cell Biol*. 35:1777-1787.

Lang, G., J. Bonnet, D. Umlauf, K. Karmodiya, J. Koffler, M. Stierle, D. Devys, and L. Tora. 2011. The Tightly Controlled Deubiquitination Activity of the Human SAGA Complex Differentially Modifies Distinct Gene Regulatory Elements. *Molecular and Cellular Biology*. 31:3734-3744.

Latouche, M., C. Lasbleiz, E. Martin, V. Monnier, T. Debeir, A. Mouatt-Prigent, M.-P. Muriel, L. Morel, M. Ruberg, A. Brice, G. Stevanin, and H. Tricoire. 2007. A Conditional Pan-Neuronal Drosophila Model of Spinocerebellar Ataxia 7 with a Reversible Adult Phenotype Suitable for Identifying Modifier Genes . *The Journal of Neuroscience*. 27:2483-2492.

Lee, H.G., J. Jo, H.H. Hong, K.K. Kim, J.K. Park, S.J. Cho, and C. Park. 2016. State-of-the-art housekeeping proteins for quantitative western blotting: Revisiting the first draft of the human proteome. *Proteomics*. 16:1863-1867.

Lee, K.K., M.E. Sardiu, S.K. Swanson, J.M. Gilmore, M. Torok, P.A. Grant, L. Florens, J.L. Workman, and M.P. Washburn. 2011a. Combinatorial depletion analysis to assemble the network architecture of the SAGA and ADA chromatin remodeling complexes. *Molecular Systems Biology*. 7:503-503.

Lee, K.K., M.E. Sardiu, S.K. Swanson, J.M. Gilmore, M. Torok, P.A. Grant, L. Florens, J.L. Workman, and M.P. Washburn. 2011b. Combinatorial depletion analysis to assemble the network architecture of the SAGA and ADA chromatin remodeling complexes. *Molecular Systems Biology*. 7.

Lee, K.K., S.K. Swanson, L. Florens, M.P. Washburn, and J.L. Workman. 2009. Yeast Sgf73/Ataxin-7 serves to anchor the deubiquitination module into both SAGA and Slik(SALSA) HAT complexes. *Epigenetics Chromatin*. 2:2.

Li, C., T. Irrazabal, C.C. So, M. Berru, L. Du, E. Lam, A.K. Ling, J.L. Gommerman, Q. Pan-Hammarstrom, and A. Martin. 2018. The H2B deubiquitinase Usp22 promotes antibody class switch recombination by facilitating non-homologous end joining. *Nat Commun*. 9:1006.

Lim, S., J. Kwak, M. Kim, and D. Lee. 2013. Separation of a functional deubiquitylating module from the SAGA complex by the proteasome regulatory particle. *Nat Commun*. 4:2641.

Ma, J., K.J. Brennan, M.R. D'Aloia, P.E. Pascuzzi, and V.M. Weake. 2016. Transcriptome Profiling Identifies Multiplexin as a Target of SAGA Deubiquitinase Activity in Glia Required for Precise Axon Guidance During Drosophila Visual Development. *G3 (Bethesda)*. 6:2435-2445.

Martin, J.J. 2012. Spinocerebellar ataxia type 7. *Handbook of clinical neurology*. 103:475-491.

Martin, K.A., B. Poeck, H. Roth, A.J. Ebens, L.C. Ballard, and S.L. Zipursky. 1995. Mutations disrupting neuronal connectivity in the Drosophila visual system. *Neuron*. 14:229-240.

McCormick, M.A., A.G. Mason, S.J. Guyenet, W. Dang, R.M. Garza, M.K. Ting, R.M. Moller, S.L. Berger, M. Kaeberlein, L. Pillus, A.R. La Spada, and B.K. Kennedy. 2014. The SAGA histone deubiquitinase module controls yeast replicative lifespan via Sir2 interaction. *Cell reports*. 8:477-486.

Meyer, G., and E.L. Feldman. 2002. Signaling mechanisms that regulate actin-based motility processes in the nervous system. *Journal of neurochemistry*. 83:490-503.

Miyamoto, K., M. Teperek, K. Yusa, G.E. Allen, C.R. Bradshaw, and J.B. Gurdon. 2013. Nuclear Wave1 is required for reprogramming transcription in oocytes and for normal development. *Science*. 341:1002-1005.

Mohan, M., H.M. Herz, Y.H. Takahashi, C. Lin, K.C. Lai, Y. Zhang, M.P. Washburn, L. Florens, and A. Shilatifard. 2010. Linking H3K79 trimethylation to Wnt signaling through a novel Dot1-containing complex (DotCom). *Genes & development*. 24:574-589.

Mohan, R.D., S.M. Abmayr, and J.L. Workman. 2014a. The expanding role for chromatin and transcription in polyglutamine disease. *Curr Opin Genet Dev*. 26:96-104.

Mohan, R.D., G. Dialynas, V.M. Weake, J. Liu, S. Martin-Brown, L. Florens, M.P. Washburn, J.L. Workman, and S.M. Abmayr. 2014b. Loss of Drosophila Ataxin-7, a SAGA subunit, reduces H2B ubiquitination and leads to neural and retinal degeneration. *Genes & development*. 28:259-272.

Navarro-Lerida, I., T. Pellinen, S.A. Sanchez, M.C. Guadamillas, Y. Wang, T. Mirtti, E. Calvo, and M.A. Del Pozo. 2015. Rac1 nucleocytoplasmic shuttling drives nuclear shape changes and tumor invasion. *Developmental cell*. 32:318-334.

Petrucelli, L., and T. Dawson. 2004. Mechanism of neurodegenerative disease: role of the ubiquitin proteasome system. *Annals of Medicine*. 36:315-320.

Poeck, B., S. Fischer, D. Gunning, S.L. Zipursky, and I. Salecker. 2001. Glial cells mediate target layer selection of retinal axons in the developing visual system of Drosophila. *Neuron*. 29:99-113.

Pollard, T.D., and C.C. Beltzner. 2002. Structure and function of the Arp2/3 complex. *Current opinion in structural biology*. 12:768-774.

Rabinovich, D., O. Mayseless, and O. Schuldiner. 2015. Long term ex vivo culturing of Drosophila brain as a method to live image pupal brains: insights into the cellular mechanisms of neuronal remodeling. *Front Cell Neurosci*. 9:327.

Ranjini Prithviraj, S.T., and Edward Giniger 2012. Ex vivo Culturing of Whole, Developing Drosophila Brains. *JOVE*.

Rawe, V.Y., C. Payne, C. Navara, and G. Schatten. 2004. WAVE1 intranuclear trafficking is essential for genomic and cytoskeletal dynamics during fertilization: cell-cycle-dependent shuttling between M-phase and interphase nuclei. *Developmental biology*. 276:253-267.

Ristic, G., W.L. Tsou, and S.V. Todi. 2014. An optimal ubiquitin-proteasome pathway in the nervous system: the role of deubiquitinating enzymes. *Front Mol Neurosci*. 7:72.

Romero-Calvo, I., B. Ocón, P. Martínez-Moya, M.D. Suárez, A. Zarzuelo, O. Martínez-Augustin, and F.S. de Medina. 2010. Reversible Ponceau staining as a loading control alternative to actin in Western blots. *Analytical Biochemistry*. 401:318-320.

Samara, N.L., A.B. Datta, C.E. Berndsen, X. Zhang, T. Yao, R.E. Cohen, and C. Wolberger. 2010a. Structural Insights into the Assembly and Function of the SAGA Deubiquitinating Module. *Science*. 328:1025.

Samara, N.L., A.B. Datta, C.E. Berndsen, X. Zhang, T. Yao, R.E. Cohen, and C. Wolberger. 2010b. Structural insights into the assembly and function of the SAGA deubiquitinating module. *Science*. 328:1025-1029.

Setiaputra, D., J.D. Ross, S. Lu, D.T. Cheng, M.Q. Dong, and C.K. Yip. 2015. Conformational flexibility and subunit arrangement of the modular yeast Spt-Ada-Gcn5 acetyltransferase complex. *J Biol Chem*. 290:10057-10070.

Suganuma, T., J.L. Gutierrez, B. Li, L. Florens, S.K. Swanson, M.P. Washburn, S.M. Abmayr, and J.L. Workman. 2008. ATAC is a double histone acetyltransferase complex that stimulates nucleosome sliding. *Nature structural & molecular biology*. 15:364-372.

Suganuma, T., A. Mushegian, S.K. Swanson, S.M. Abmayr, L. Florens, M.P. Washburn, and J.L. Workman. 2010. The ATAC Acetyltransferase Complex Coordinates MAP Kinases to Regulate JNK Target Genes. *Cell*. 142:726-736.

Takenawa, T., and H. Miki. 2001. WASP and WAVE family proteins: key molecules for rapid rearrangement of cortical actin filaments and cell movement. *Journal of Cell Science*. 114:1801-1809.

Taylor, M.D., S. Sadhukhan, P. Kottangada, A. Ramgopal, K. Sarkar, S. D'Silva, A. Selvakumar, F. Candotti, and Y.M. Vyas. 2010. Nuclear role of WASp in the pathogenesis of dysregulated TH1 immunity in human Wiskott-Aldrich syndrome. *Science translational medicine*. 2:37ra44.

Tran, D.T., A. Masedunskas, R. Weigert, and K.G. Ten Hagen. 2015. Arp2/3-mediated F-actin formation controls regulated exocytosis in vivo. *Nat Commun*. 6:10098.

Tsou, W.L., M.J. Sheedlo, M.E. Morrow, J.R. Blount, K.M. McGregor, C. Das, and S.V. Todi. 2012. Systematic analysis of the physiological importance of deubiquitinating enzymes. *PLoS One*. 7:e43112.

Ui-Tei, K., S. Nishihara, M. Sakuma, K. Matsuda, T. Miyake, and Y. Miyata. 1994. Chemical analysis of neurotransmitter candidates in clonal cell lines from Drosophila central nervous system. I. ACh and L-dopa. *Neurosci Lett*. 174:85-88.

Ui-Tei, K., M. Sakuma, Y. Watanabe, T. Miyake, and Y. Miyata. 1995. Chemical analysis of neurotransmitter candidates in clonal cell lines from Drosophila central nervous system, II: Neuropeptides and amino acids. *Neurosci Lett*. 195:187-190.

Ui, K., S. Nishihara, M. Sakuma, S. Togashi, R. Ueda, Y. Miyata, and T. Miyake. 1994. Newly established cell lines from Drosophila larval CNS express neural specific characteristics. *In vitro cellular & developmental biology. Animal*. 30a:209-216.

van der Knaap, J.A., E. Kozhevnikova, K. Langenberg, Y.M. Moshkin, and C.P. Verrijzer. 2010. Biosynthetic enzyme GMP synthetase cooperates with ubiquitin-specific protease 7 in transcriptional regulation of ecdysteroid target genes. *Molecular and Cellular Biology*. 30:736-744.

van der Knaap, J.A., B.R. Kumar, Y.M. Moshkin, K. Langenberg, J. Krijgsveld, A.J. Heck, F. Karch, and C.P. Verrijzer. 2005. GMP synthetase stimulates histone H2B deubiquitylation by the epigenetic silencer USP7. *Molecular Cell*. 17:695-707.

Verboon, J.M., and S.M. Parkhurst. 2015. Rho family GTPase functions in Drosophila epithelial wound repair. *Small GTPases*. 6:28-35.

Verboon, J.M., H. Rincon-Arano, T.R. Werwie, J.J. Delrow, D. Scalzo, V. Nandakumar, M. Groudine, and S.M. Parkhurst. 2015. Wash interacts with lamin and affects global nuclear organization. *Curr Biol*. 25:804-810.

Vishavkarma, R., S. Raghavan, C. Kuyyamudi, A. Majumder, J. Dhawan, and P.A. Pullarkat. 2014. Role of Actin Filaments in Correlating Nuclear Shape and Cell Spreading. *PLOS ONE*. 9:e107895.

Washburn, M.P., D. Wolters, and J.R. Yates, 3rd. 2001. Large-scale analysis of the yeast proteome by multidimensional protein identification technology. *Nat Biotechnol*. 19:242-247.

Weake, V.M., K.K. Lee, S. Guelman, C.H. Lin, C. Seidel, S.M. Abmayr, and J.L. Workman. 2008. SAGA-mediated H2B deubiquitination controls the development of neuronal connectivity in the Drosophila visual system. *EMBO J*. 27:394-405.

Yang, H., S. Liu, W.T. He, J. Zhao, L.L. Jiang, and H.Y. Hu. 2015. Aggregation of Polyglutamine-expanded Ataxin 7 Protein Specifically Sequesters Ubiquitin-specific Protease 22 and Deteriorates Its Deubiquitinating Function in the Spt-Ada-Gcn5-Acetyltransferase (SAGA) Complex. *J Biol Chem*. 290:21996-22004.

Yoo, Y., X. Wu, and J.L. Guan. 2007. A novel role of the actin-nucleating Arp2/3 complex in the regulation of RNA polymerase II-dependent transcription. *J Biol Chem*. 282:7616-7623.

Young, J.E., L. Gouw, S. Propp, B.L. Sopher, J. Taylor, A. Lin, E. Hermel, A. Logvinova, S.F. Chen, S. Chen, D.E. Bredesen, R. Truant, L.J. Ptacek, A.R. La Spada, and L.M. Ellerby. 2007. Proteolytic cleavage of ataxin-7 by caspase-7 modulates cellular toxicity and transcriptional dysregulation. *J Biol Chem*. 282:30150-30160.

Yu, C., K.H. Wan, A.S. Hammonds, M. Stapleton, J.W. Carlson, and S.E. Celniker. 2011. Development of expression-ready constructs for generation of proteomic libraries. *Methods in molecular biology*. 723:257-272.

Zallen, J.A., Y. Cohen, A.M. Hudson, L. Cooley, E. Wieschaus, and E.D. Schejter. 2002. SCAR is a primary regulator of Arp2/3-dependent morphological events in Drosophila. *Journal of Cell Biology*. 156:689-701.

Zhang, Y., Z. Wen, M.P. Washburn, and L. Florens. 2010. Refinements to label free proteome quantitation: how to deal with peptides shared by multiple proteins. *Analytical chemistry*. 82:2272-2281.

Zhao, Y., G. Lang, S. Ito, J. Bonnet, E. Metzger, S. Sawatsubashi, E. Suzuki, X. Le Guezennec, H.G. Stunnenberg, A. Krasnov, S.G. Georgieva, R. Schule, K. Takeyama, S. Kato, L. Tora, and D. Devys. 2008. A TFTC/STAGA module mediates histone H2A and H2B deubiquitination, coactivates nuclear receptors, and counteracts heterochromatin silencing. *Mol Cell*. 29:92-101.

Figure 1

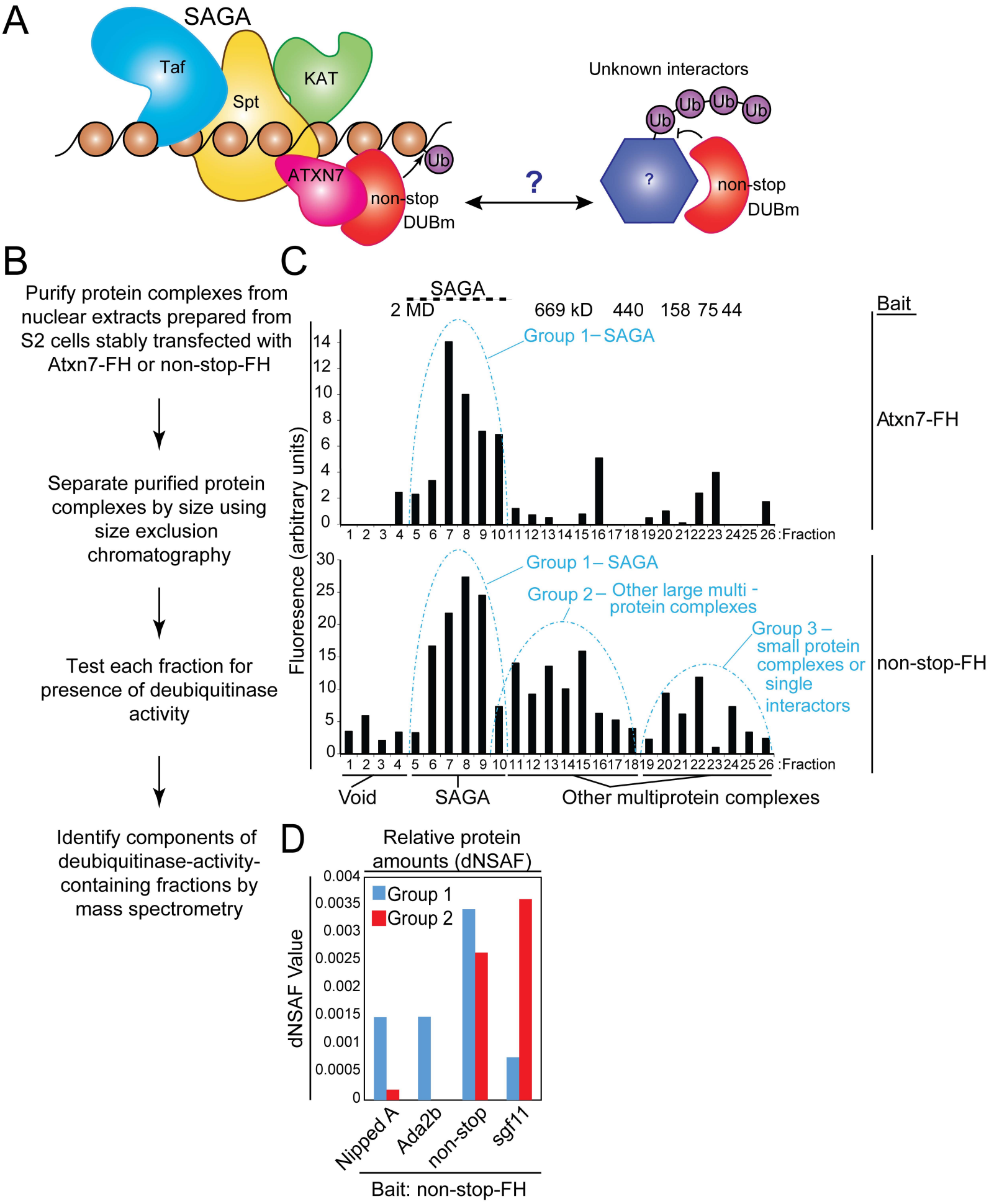
A
SAGA
Taf
Spt
KAT
ATXN7
non-stop
DUBm
Ub
?
Unknown interactors
Ub
Ub
Ub
Ub
?
non-stop
DUBm
B
Purify protein complexes from nuclear extracts prepared from S2 cells stably transfected with Atxn7-FH or non-stop-FH
Separate purified protein complexes by size using size exclusion chromatography
Test each fraction for presence of deubiquitinase activity
Identify components of deubiquitinase-activity-containing fractions by mass spectrometry
C
SAGA
2 MD
669 kD
440
158
75
44
Bait
Group 1– SAGA
Atxn7-FH
Fluoresence (arbitrary units)
:Fraction
Group 1– SAGA
Group 2 – Other large multi - protein complexes
Group 3 – small protein complexes or single interactors
non-stop-FH
Void
SAGA
Other multiprotein complexes
D
Relative protein amounts (dNSAF)
Group 1
Group 2
dNSAF Value
Nipped A
Ada2b
non-stop
sgf11
Bait: non-stop-FH

Figure 2

A

Protein name		Total input				non-stop "Group 2" fraction				Vector only control		
Description	NCBI_Gene	Spectra	Sequence coverage	dNSAF		Spectra	Sequence coverage	dNSAF		Spectra	Sequence coverage	dNSAF
Sgf11	Sgf11	7	12.2	8.1E-4		2	8.7	7.7E-4		0	0	0
enhancer of yellow 2	e(y)2	19	17.8	4.3E-3		15	25.7	1.1E-2		0	0	0
Non-stop	not	51	20.2	1.6E-3		32	15.7	3.4E-3		0	0	0
histone H2A	His2A	75	25.8	1.4E-2		40	31.5	2.4E-2		0	0	0
histone H2B	His2B	30	26.8	5.5E-3		1	7.3	6.1E-4		0	0	0
Actin-related protein 3	Arp3	39	34.7	2.1E-3		20	31.1	3.6E-3		0	0	0
Arpc3A, isoform C	Arpc3A	31	11.9	4.0E-3		14	21.5	6.0E-3		0	0	0
Arpc2	Arpc2	37	16.0	2.8E-3		5	12.3	1.3E-3		0	0	0
Arpc4	Arpc4	5	18.5	6.8E-4		7	19.1	3.1E-3		0	0	0
Arpc3B, isoform B	Arpc3b	1	8.9	1.4E-4		1	13.4	4.8E-4		0	0	0
Actin-related protein 2	Arp2	3	3.65	1.7E-4		4	3.6	7.7E-3		0	0	0
suppressor of profilin 2	Sop2	3	7.2	1.8E-4		9	14.3	1.8E-3		0	0	0
Arpc5	Arpc5	13	37.8	2.0E-3		7	24.5	3.5E-3		0	0	0
SCAR	SCAR	0	0	0		2	2.2	2.5E-4		0	0	0
HEM-protein	Hem	2	1.1	4.0E-5		1	1.1	4.3E-5		0	0	0
SRA-1	Sra-1	2	1.1	1.2E-4		4	2.2	1.5E-4		0	0	0

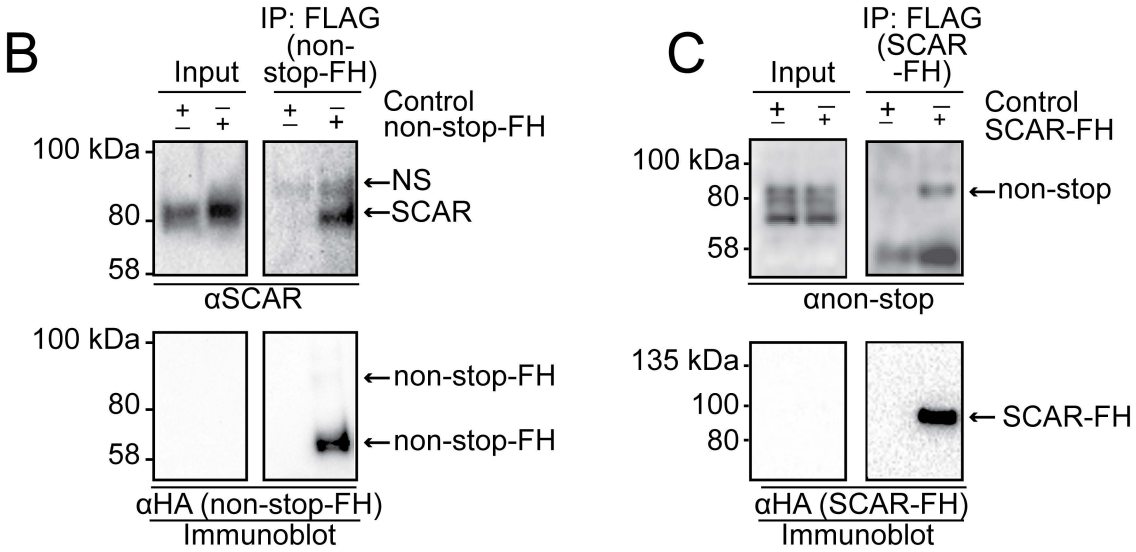

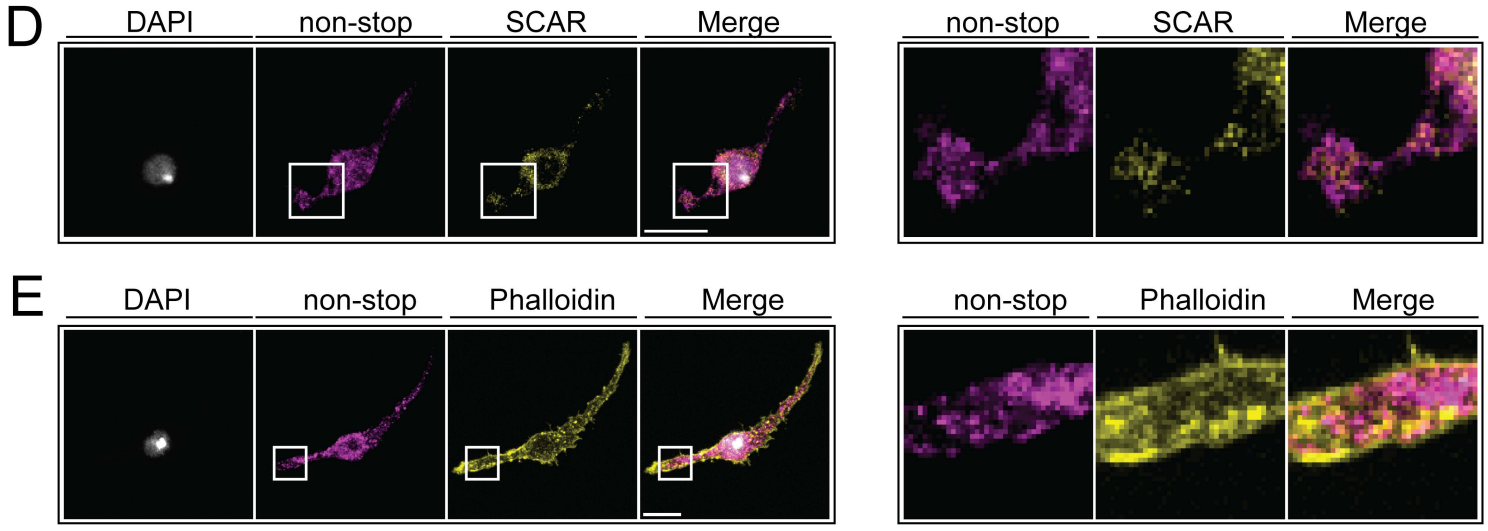

Figure 3

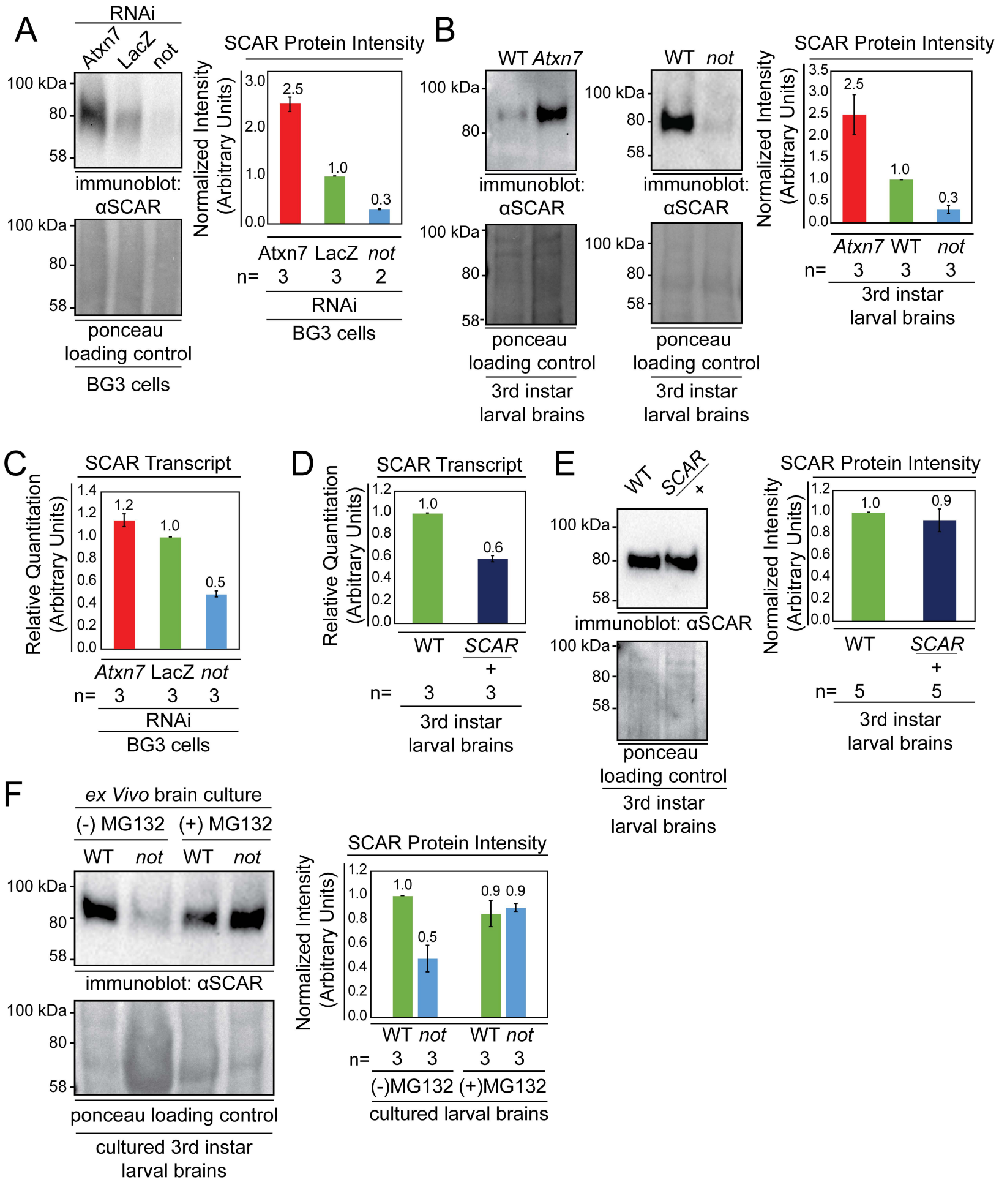
A
RNAi
Atxn7
LacZ
not
100 kDa
80
58
immunoblot: αSCAR
ponceau loading control
BG3 cells
SCAR Protein Intensity
Normalized Intensity (Arbitrary Units)
2.5
1.0
0.3
Atxn7 LacZ not
n= 3 3 2
RNAi
BG3 cells
B
WT Atxn7
WT not
immunoblot: αSCAR
ponceau loading control
3rd instar larval brains
SCAR Protein Intensity
Atxn7 WT not
n= 3 3 3
C
SCAR Transcript
Relative Quantitation (Arbitrary Units)
1.2
1.0
0.5
Atxn7 LacZ not
n= 3 3 3
RNAi
BG3 cells
D
SCAR Transcript
1.0
0.6
WT SCAR +
n= 3 3
3rd instar larval brains
E
WT
SCAR +
immunoblot: αSCAR
ponceau loading control
3rd instar larval brains
SCAR Protein Intensity
1.0
0.9
WT SCAR +
n= 5 5
3rd instar larval brains
F
ex Vivo brain culture
(-) MG132
(+) MG132
WT not WT not
immunoblot: αSCAR
ponceau loading control
cultured 3rd instar larval brains
SCAR Protein Intensity
1.0
0.5
0.9 0.9
WT not WT not
n= 3 3 3 3
(-)MG132 (+)MG132
cultured larval brains

Figure 4

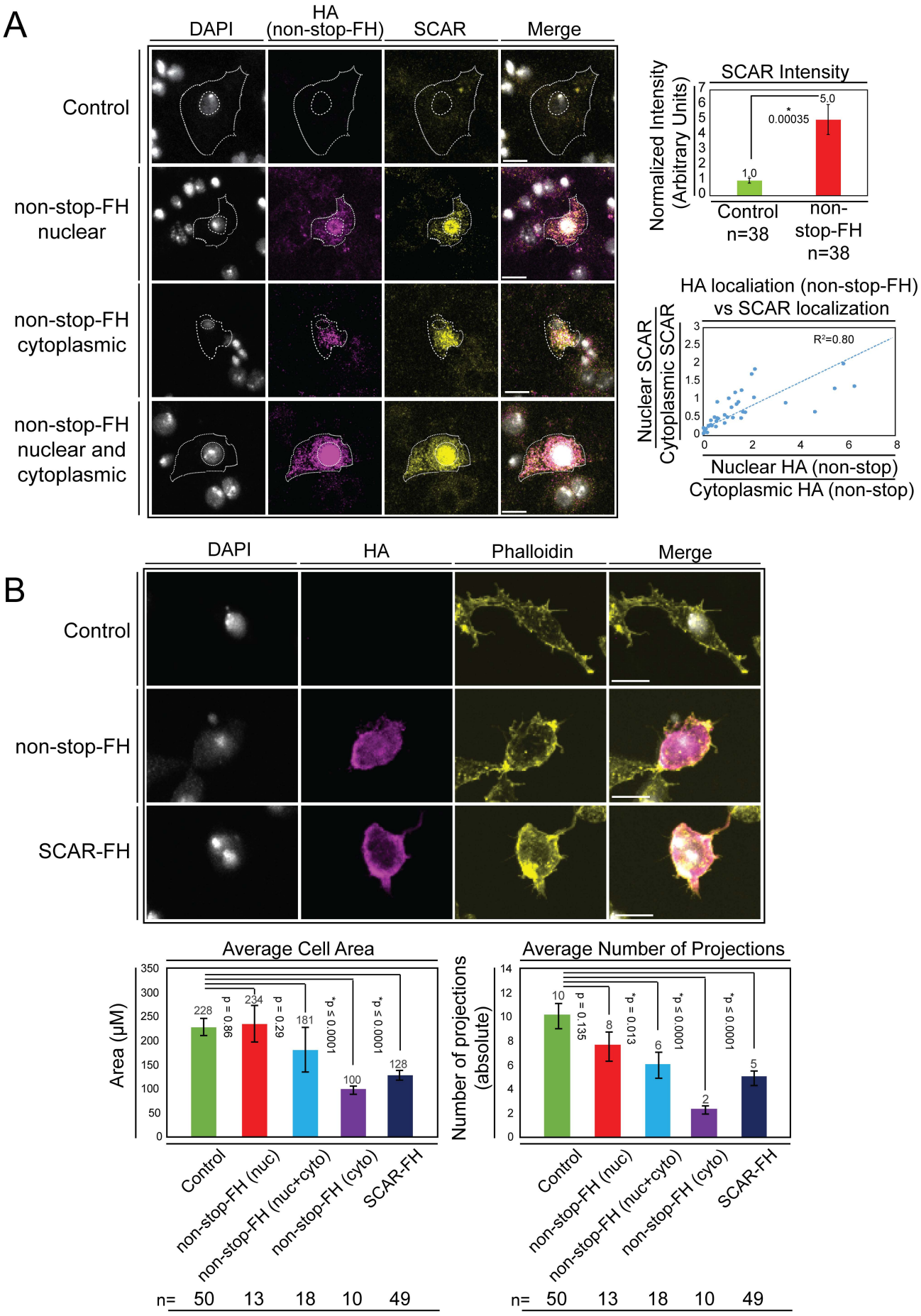
A
DAPI
HA (non-stop-FH)
SCAR
Merge
Control
non-stop-FH nuclear
non-stop-FH cytoplasmic
non-stop-FH nuclear and cytoplasmic
SCAR Intensity
Normalized Intensity (Arbitrary Units)
5.0
*
0.00035
1.0
Control n=38
non-stop-FH n=38
HA localiation (non-stop-FH) vs SCAR localization
Nuclear SCAR / Cytoplasmic SCAR
R²=0.80
Nuclear HA (non-stop) / Cytoplasmic HA (non-stop)
B
DAPI
HA
Phalloidin
Merge
Control
non-stop-FH
SCAR-FH
Average Cell Area
Area (µM)
228
234
181
100
128
p = 0.86
p = 0.29
*p ≤ 0.0001
*p ≤ 0.0001
Control
non-stop-FH (nuc)
non-stop-FH (nuc+cyto)
non-stop-FH (cyto)
SCAR-FH
n= 50 13 18 10 49
Average Number of Projections
Number of projections (absolute)
10
8
6
2
5
p = 0.135
*p = 0.013
*p ≤ 0.0001
*p ≤ 0.0001
Control
non-stop-FH (nuc)
non-stop-FH (nuc+cyto)
non-stop-FH (cyto)
SCAR-FH
n= 50 13 18 10 49

Figure 5

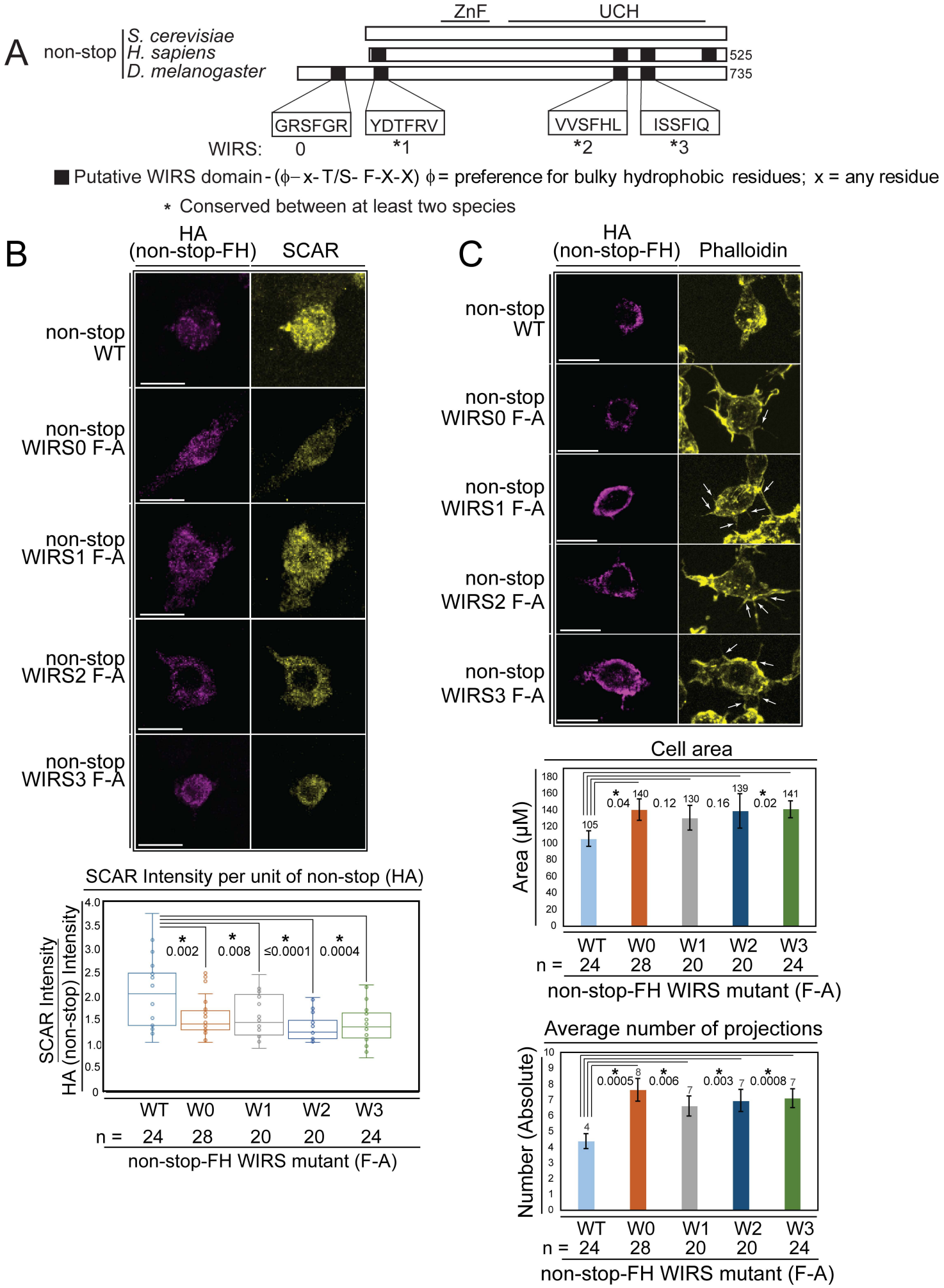
A
non-stop
S. cerevisiae
H. sapiens
D. melanogaster
ZnF
UCH
525
735
GRSFGR
YDTFRV
VVSFHL
ISSFIQ
WIRS: 0 *1 *2 *3
Putative WIRS domain - (ϕ– x- T/S- F-X-X) ϕ = preference for bulky hydrophobic residues; x = any residue
* Conserved between at least two species
B
HA (non-stop-FH)
SCAR
non-stop WT
non-stop WIRS0 F-A
non-stop WIRS1 F-A
non-stop WIRS2 F-A
non-stop WIRS3 F-A
SCAR Intensity per unit of non-stop (HA)
SCAR Intensity / HA (non-stop) Intensity
* 0.002
* 0.008
* ≤0.0001
* 0.0004
WT W0 W1 W2 W3
n = 24 28 20 20 24
non-stop-FH WIRS mutant (F-A)
C
HA (non-stop-FH)
Phalloidin
non-stop WT
non-stop WIRS0 F-A
non-stop WIRS1 F-A
non-stop WIRS2 F-A
non-stop WIRS3 F-A
Cell area
Area (μM)
105
* 0.04
140
0.12
130
0.16
139
* 0.02
141
WT W0 W1 W2 W3
n = 24 28 20 20 24
non-stop-FH WIRS mutant (F-A)
Average number of projections
Number (Absolute)
4
* 0.0005
8
* 0.006
7
* 0.003
7
* 0.0008
7
WT W0 W1 W2 W3
n = 24 28 20 20 24
non-stop-FH WIRS mutant (F-A)

Figure 6

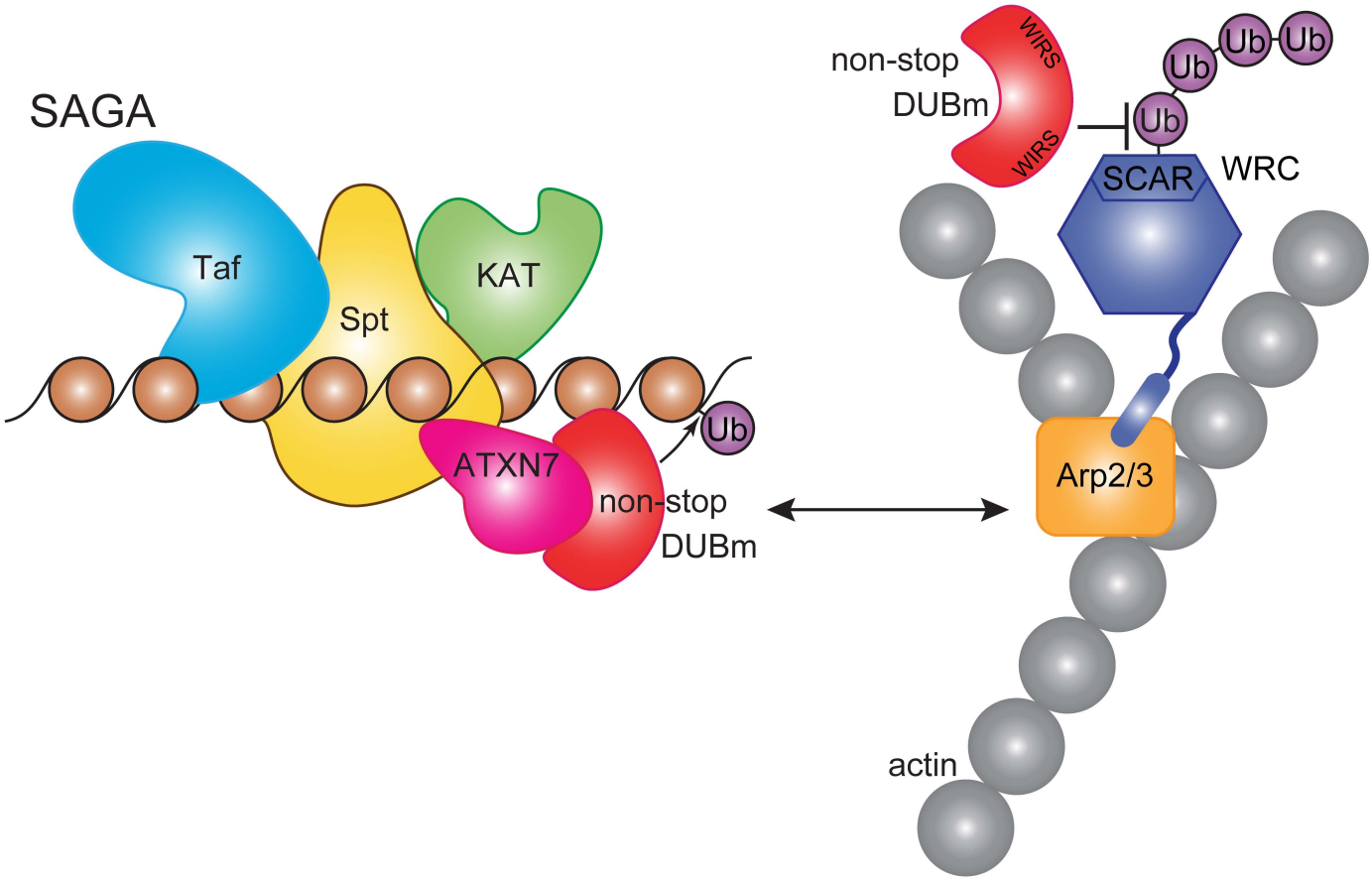
SAGA
Taf
Spt
KAT
ATXN7
non-stop
DUBm
Ub
non-stop
DUBm
WIRS
WIRS
Ub
Ub
Ub
Ub
SCAR
WRC
Arp2/3
actin